

**Syntheses of Oligosaccharide Analogues as Molecular  
Probes for Mechanistic Investigation of  
Endoglycosidases**

**Kazunori Yamamoto**

**2009**

**The United Graduate School of Agricultural Sciences, Iwate University**

## 謝辞

本研究を行う機会を賜り、学部4年の頃より現在まで終始一貫して、研究の内容や方針について多大なるご指導とご助言を頂きました、弘前大学農学生命科学部教授、橋本勝先生に心より御礼申し上げます。

また、日頃より本研究を行うにあたり、さまざまなご助言を頂き、大変お世話になりました、弘前大学農学生命科学部名誉教授（現、秋田看護福祉大学教授）、奥野智旦先生、弘前大学農学生命科学部教授、宮入一夫先生、弘前大学農学生命科学部准教授、高田晃先生に心より御礼申し上げます。

スーパーコンピュータを用いた分子動力学計算を行って頂いた、弘前大学理工学部教授、斎藤稔先生に深く感謝申し上げます。

Endo-PG1のX線結晶構造について貴重なご助言を頂いた、独立行政法人理化学研究所、清水哲哉博士に心より感謝申し上げます。

合成した基質アナログのNMRの測定を行って頂き、投稿論文をまとめる際にもご助言、ご協力を頂きました、産業技術総合研究所、清水弘樹博士に深く御礼申し上げます。

セルラーゼに関するご助言を頂き、基質アナログの活性測定を行って頂きました、長岡技術科学大学准教授、城所俊一先生に心より感謝申し上げます。

質量スペクトルの測定を行って頂きました北海道大学農学研究院教授、川端潤先生、北海道大学農学部 GC-MS & NMR室、福士江里博士に深く感謝申し上げます。

また、学会などでお会いする度に、気にかけていただき、ご助言頂きました帯広畜産大学准教授、橋本誠先生に心より御礼申し上げます。

表面プラズモン共鳴の測定を行って頂いた新谷智行修士に心より感謝申し上げます。

本研究を始めるにあたり、ご指導、ご助言頂いた、松田寛子博士、大原啓一郎博士、藤田純次修士、森井康晴修士をはじめとする研究室の諸先輩方に深く感謝申し上げます。

また、共に研究を進めてきた、渡辺直樹氏、荒添圭朗修士、佐藤佑修士、江下僚氏、石森歩氏、工藤慎士氏、野口翔悟氏をはじめとする生物化学研究室の皆様にご心より感謝申し上げます。特に、研究室での6年間、研究だけでなく、様々な面で私を支えてくださった、村上貴宣博士に深く感謝申し上げます。

なお、本研究の一部は文部科学省科学研究費、弘前大学学長指定重点研究費の補助のもと行われました。

## **Index**

<b>Chapter 1</b>	<b>Introduction</b>	page 1
<b>Chapter 2</b>	<b>Trigalacturonic acid analogues as molecular probes for mechanistic investigation of endo-polygalacturonase1 (endo-PG1)</b>	page 9
2.1	Introduction of this chapter	page 10
2.2	Synthesis of trigalacturonic acid methylglycoside	page 13
2.3	Synthesis of sulfur substituted analogue	page 19
2.3.1	Design prior to the synthesis	page 19
2.3.2	Synthesis	page 20
2.3.3	Biological property of sulfur substituted analogue	page 27
2.3.4	Conformational analysis	page 28
2.4	Synthesis of transition state analogue	page 31
<b>Chapter 3</b>	<b>Cellotriose analogues as molecular probes for mechanistic investigation of cellulase</b>	page 40
3.1	Introduction of this Chapter	page 41
3.2	Syntheses of sulfur substituted analogues	page 43
3.3	Syntheses of transition state analogues	page 45
<b>Chapter 4</b>	<b>Conclusion</b>	page 52
<b>Chapter 5</b>	<b>Experimental Section</b>	page 55
	<b>References and notes</b>	Page 175
<b>Chapter 6</b>	<b><math>^1\text{H}</math> and <math>^{13}\text{C}</math> NMR spectra for novel compounds appeared in this thesis</b>	page 180

**Chapter 1.**  
**Introduction**

The glycosidases catalyze hydrolysis of the carbohydrate chains which exist as amylose, amylopectin, cellulose and so on. Since some oligosaccharides given by these processes showed valuable biological properties for health supplements and useful properties as gellents, productions of oligosaccharides are now attracted much attention not only in biological science but also in food and material industries. In other word, understanding the detailed reaction mechanisms of enzymatic glycolysis is indispensable in these fields.

Glycosidases are classified in two types exo-glycosidases and endo-glycosidases, based on their characters as shown in **Figure i-1**. Exo-glycosidases hydrolyze non-reducing end (sometimes the second or third glycosidyl linkages from the non-reducing end) of glycoside bonds of the carbohydrate chains. These recognize the structural and electropotential

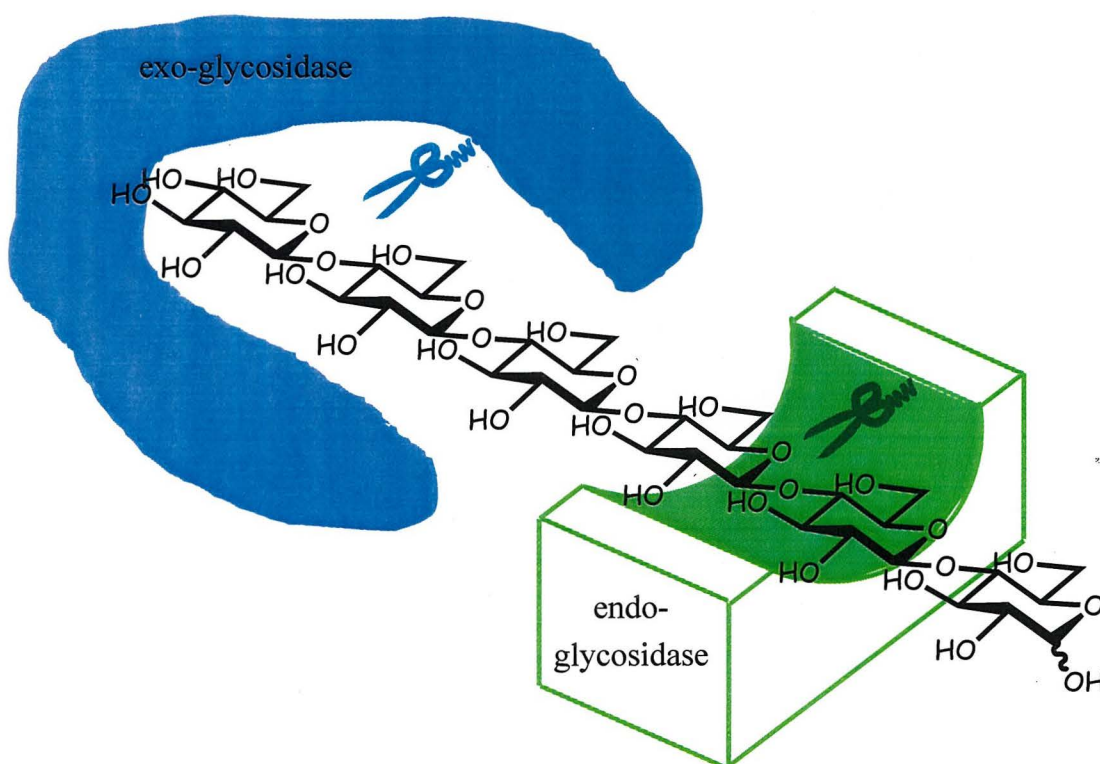


**Figure i-1.** A mode of hydrolysis of exo- and endo-glycosidase

properties of carbohydrate on the non-reducing end. So, many of inhibitors for exo-glycosidases have been developed such as acarbose (**i-1**),<sup>1</sup> deoxynojirimycin (**i-2**),<sup>2, 3</sup> and voglibose (**i-3**),<sup>4, 5</sup> with aims studying of the enzymatic reaction mechanism or medicinal usages (**Figure i-2**). Some natural products such as swainsonin (**i-4**)<sup>6</sup> are now also under clinical usage.

On the other hand, endo-glycosidases hydrolyze the internal glycoside bonds of a long carbohydrate chain (see **Figure i-1**). This type of glycosidases only recognize the sequence of the sugar chain, accordingly these can slide over the carbohydrate chain. This property has brought us difficulty in making homogeneous complexes between the enzyme and their inhibitors. These facts have made the reaction mechanistic studies behind compare to those of exo-glycosidases.

The author planed to develop carbohydrate analogues effective for the mechanistic studies. Carbohydrate mimics called carbomimetics would be ideal

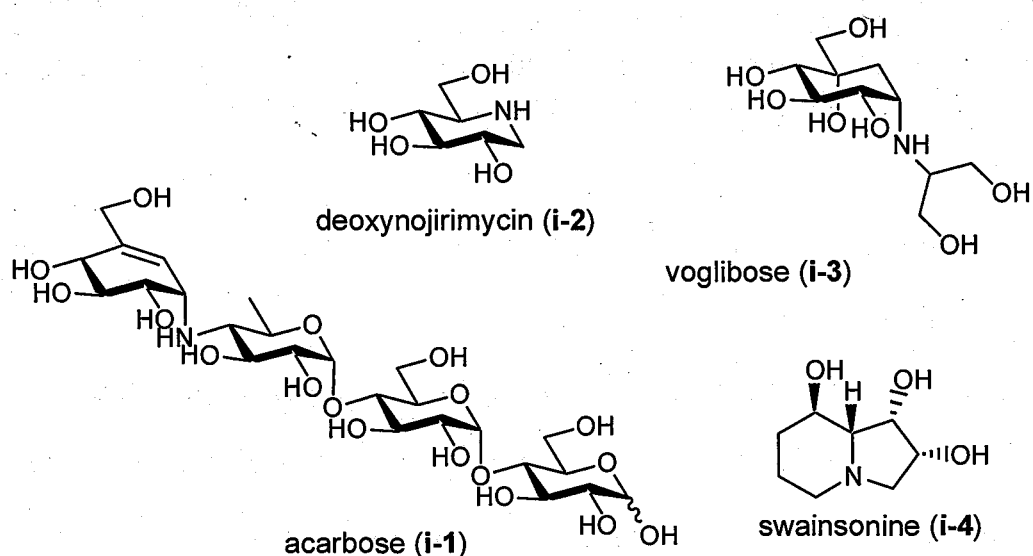


**Figure i-2.** Inhibitors for exo-glycosidases.

in this purpose. Since we need to observe the enzyme/probe complex in these studies, the probe must stay on the glycosidases without cleaving.<sup>7</sup> It is well known the substrate saccharide chains are nicely incorporated into the glycosidases, these should be immediately degraded and released. So the probes must be stable against the enzyme. Additionally, minimum structural alterations

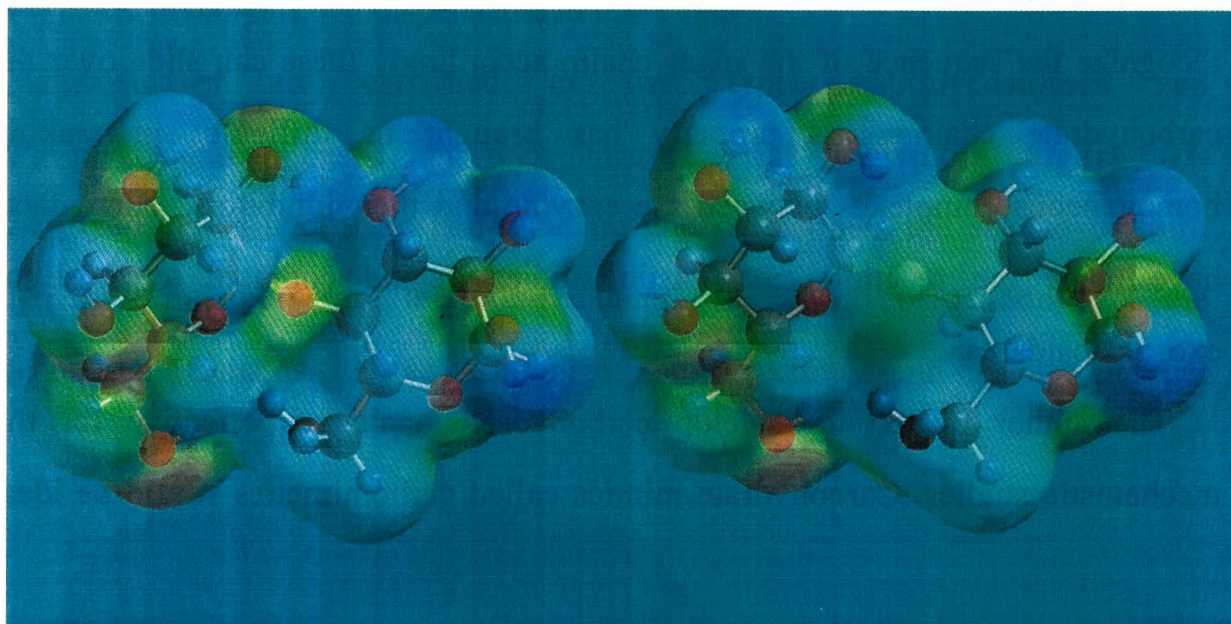


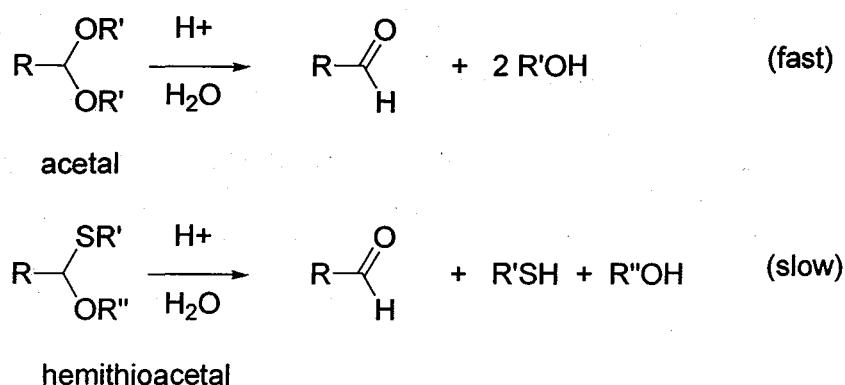
**Figure i-3.** Stable structures and distributions of electron potential of amylose (*left*) and thioamylose (*right*) obtained by AM1 calculations.

from the natural substrate should be preferable in the mechanistic studies after the complexations.

Since, oxygen and sulfur atoms belong to chalcogen, compounds involving these atoms have been known to show similar physical and chemical properties. For example both ether (C-O-C) and thioether (C-S-C) have bended two valences. In fact, semi-empirical AM1 calculations indicated that amylose and thioamylose, carrying sulfur atom in place of glycosidic oxygen, show very similar stable structures as well as electropotential distribution as shown in **Figure i-3**.



On the other hand, chemical properties are sometimes slightly different between the compounds containing oxygen and sulfur. It has also been known that acidic hydrolysis of hemithioacetals (consist of aldehyde, alcohol, and thiol) are very slow in spite of regular acetals (consist of aldehyde and two mols of alcohol) are hydrolyzed quickly under the same conditions (**Scheme i-1**).<sup>8</sup>



**Scheme i-1.**

The author expected replacements glycosidic oxygen atom at the reaction site of oligosaccharides with sulfur would realize resistibility against glycosidases with minimum structural alteration. Since these thiosaccharides should take similar structure as the natural carbohydrates to minimize the disarrangement of the hydrogen bonding network between the mimic and the glycosidases at the substance recognizing sites, these were expected to provide the ideal complex with the glycosidases in these purposes. Since these thiosaccharides mimic the stable conformation of the substrates, these might reproduce the early stage of the enzymatic reactions.

Glycosidases catalyze the hydrolysis of glycosides. It is well known catalysts involving enzymes stabilize the transition states of the reactions. If we reproduce the transition state using substrate mimics, it will provide more valuable information than above substrate mimics which are designed to reproduce stable structures of the substrates. In designation of transition state mimics, we need to stabilize the strained transition structures of the substrates. In other word, catalysts (enzymes) stabilize the strained transition structures. In the transition state of the glycolysis, the pyranose ring at the reaction site are expected to take the strained half-boat conformation to lead the oxocarbenium ion intermediate by releasing a proton. Since cyclohexene takes *pseudo*-half boat conformation as the stable structure (see **Figure i-4** and **Figure i-5**), the author planed stabilize the half-boat conformation of the transition state or the oxocarbenium intermediate by introducing cyclohexene ring in place of the pyranose ring. Acarbose (**i-1**) carries cyclohexene structure in the molecule. It may realize potent glycosidase

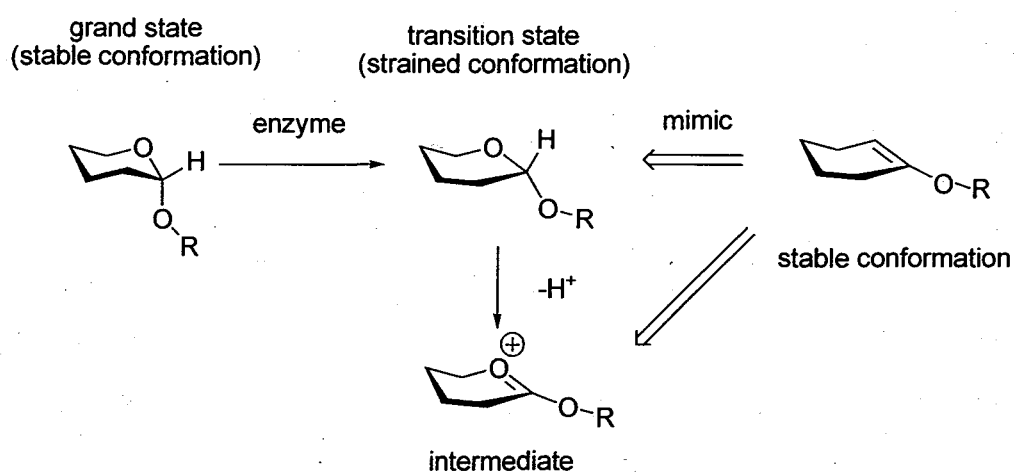


**Figure i-4.** Stabilization of the strained transition state structure.

inhibitory activity in this mechanism.

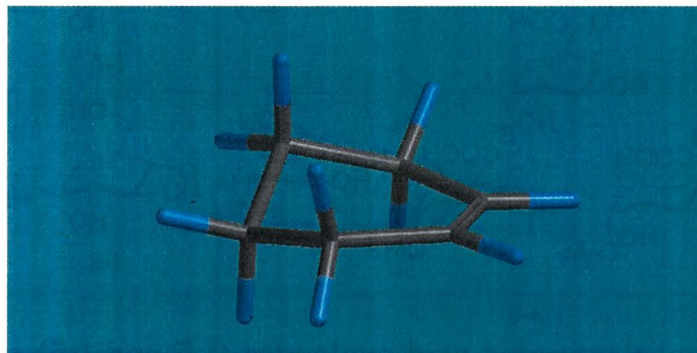


**Figure i-5.** Conformation of cyclohexene.

The author performed synthesis of these two types of oligogalacturonic acid (**i-5** and **i-6**, **Chapter 2**) as well as oligocellulose mimics (**i-7** and **i-8**, **Chapter 3**) (**Figure i-6**). The author also disclosed thiogalacturonic acid derivative (**i-5**) made complex with endo-PG1 and the life time the complex was thousand times larger than that with natural substrate. Unfortunately, sulfur substituted cellotriose (**i-7**) did not exhibit interaction with cellulase, isolated from *Humicola insolens*, cyclohexene analogue (**i-8**) made definite complex with the cellulase. The colorimetric experiments by Professor Kidokoro of Nagaoka University of Technology revealed the K value (equilibrium constant) was  $5.0 \times 10^4$  mol/L.

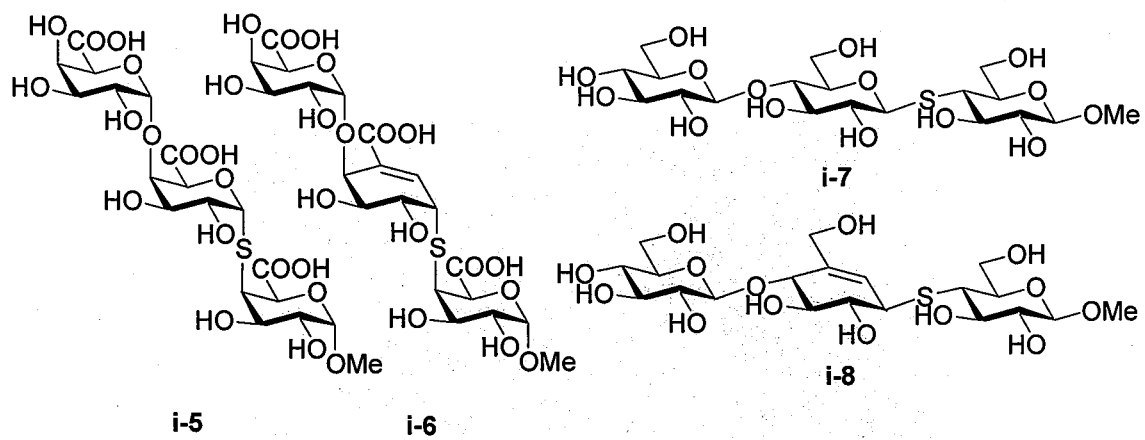


**Figure i-6.** Oligogalacturonic acid analogues (**i-5** and **i-6**) and oligocellulose analogues (**i-7** and **i-8**).

## **Chapter 2.**

### **Trigalacturonic acid analogues as molecular probes for mechanistic investigation of endo-polygalacturonase1 (endo-PG1)**

## 2.1. Introduction of this chapter

The author first performed syntheses of oligogalacturonic acid analogues (**ii-1**, **ii-2**) by focusing on endo-PG1 (PDB ID 1K5C) (**Figure ii-1**). Endo-PG1 was discovered by Professor Miyairi of Hirosaki University, one of my advisors in my doctoral course, and Emeritus Professor Okuno in 1985 from the *Stereum purpureum*<sup>9</sup> which causes silver leaf disease on apples.<sup>10</sup> They also revealed that endo-PG1 provided very nice single crystals to provide X-ray crystallographic structures with extremely high resolution.<sup>11</sup> However, the soaking experiments employing natural substrate failed in obtaining images of the complex between the enzyme and the substrate before the hydrolysis. That provided only the complex between endo-PG1 with the hydrolysate caused in the crystalline lattice due to the nature of endo-PG1 itself.<sup>12</sup> The author expected enzyme resistant



**Figure ii-1** Structure of endo-PG1 established by X-ray crystallographic analysis (PDB: 1K5C)

oligo-pactate mimic may give the complex to provide indispensable information for the reaction mechanism. Therefore the author planned to synthesize the analogues **ii-1** and **ii-2** as shown in **Figure ii-2**.

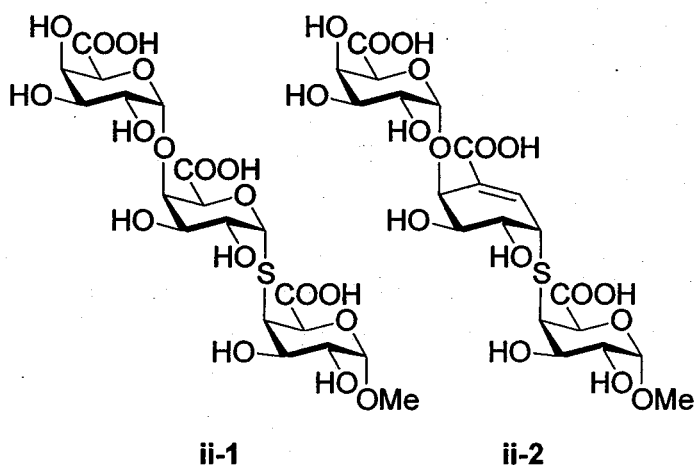


**Figure ii-2.** Structures of trigalacturonic acid analogues.

Prior to the synthesis, the author investigated the design of the suitable analogues based on the kinetic information established by Professor Miyairi.<sup>13</sup> Endo-PG1 cleaves polygalacturonic acid and the minimum size was trimer. Since the reaction rate with tetragalacturonic acid was much higher than that of the trimer, the tetramer should make more stable complex with endo-PG 1 than the trimer. As shown in **Figure ii-3**, the reaction with the tetramer cleaved the reducing end glycoside bonds predominantly to give a pair of galacturonic acid and trigalacturonic acid (90%). However, the reaction also cleave the central glycoside bond in 10% selectivity. This suggested complexation with the tetramer will provide mixture of the complexes binding with the tetramer in different site

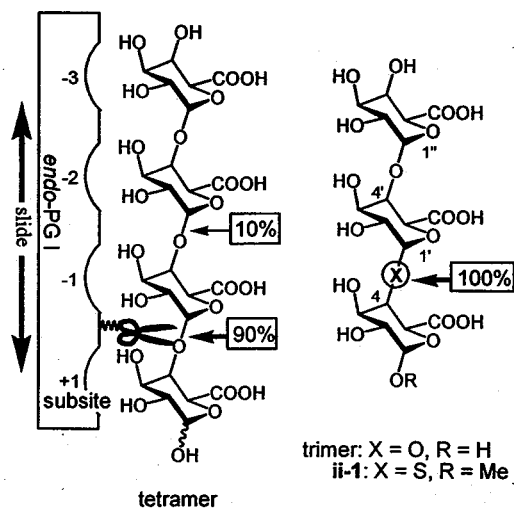


**Figure ii-3.** Site specificity in the hydrolysis by endo-PG1 in cases for tetragalacturonic acid (left) and trigelacturonic acid (right).

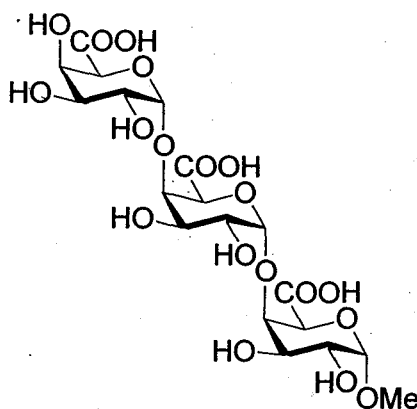
to make difficulty to obtain the homogeneous complex using the tetramer. Since trigalacturonic acid was specifically hydrolyzed the glycoside bond at the reducing end, which can make us to expected that trigalacturonic acid analogue might result homogeneous complex with endo-PG1 even the interaction was weak. Thus, the author decided to synthesize trigalacturonic acid analogue (**ii-1**) as the molecular probe. Based on information about the reaction products, sulfur atom was introduced at the glycoside bond at the reducing end.

The anomeric hydroxy group at the reducing end should cause anomerization to give mixture of  $\alpha$ - and  $\beta$ -anomers, which should bring difficulties in the thermodynamic considerations such as calorimetric experiments and analysis by molecular modeling experiments. Since the author thought thermodynamic considerations were important, the reducing terminal was fixed by introducing  $\alpha$ -methyl glycoside.



## 2.2. Synthesis of trigalacturonic acid methylglycoside (ii-3)<sup>14</sup>

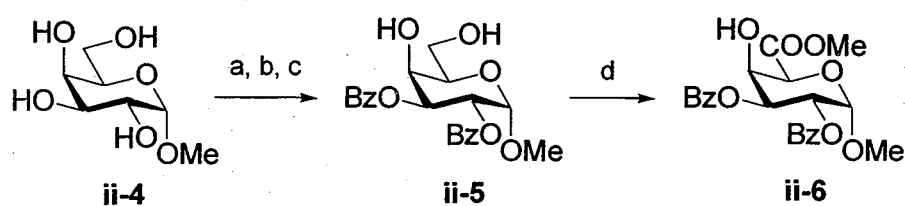
Thermodynamic discussions need the control substance to evaluate the carbomimetics evaluate **ii-1** and **ii-2**. Trigalacturonic acid is the control substance in this purpose. However, anomerization of trigalacturonic acid should occur in solution to make these discussions complex. The author set methylglycoside **ii-3** as the stable control (**Figure ii-4**). Unfortunately, **ii-3** was not known in the literature, so the author needed to prepare it by myself. The author initially attempted preparation of **ii-3** by the enzymatic partial degradation of polygalacturonic acid employing endo-PG1 and subsequent methyl glycosylation. However, all trials failed, due to the low yield in the enzymatic degradation and the isolation difficulty at the final step. The author therefore decided to prepare it by chemical synthesis.



**ii-3**

**Figure ii-4.** Trigalacturonic acid methylglycoside **ii-3** as a control substrate.

Commercial available methyl  $\alpha$ -D-galactopyranoside (**ii-4**) was converted into 4,6-diol **ii-5** by the sequential reactions of (i) tritylation of the C6 primary alcohol, (ii) benzylation using two equivalents of benzoyl chloride at low temperature, and (iii) acidic hydrolysis of the trityl ether (**Scheme ii-1**). The benzylation reaction proceeded selectively at the sterically less-hindered C2 and C3 hydroxy groups. It was found that a combination of TEMPO and  $\text{PhI}(\text{OAc})_2$ <sup>15, 16</sup> took place the regioselective oxidation of **ii-5** to give the corresponding galacturonic acid derivative which was isolated after conversion into methyl ester **ii-6** (95% yield in two steps) by using diazomethane.

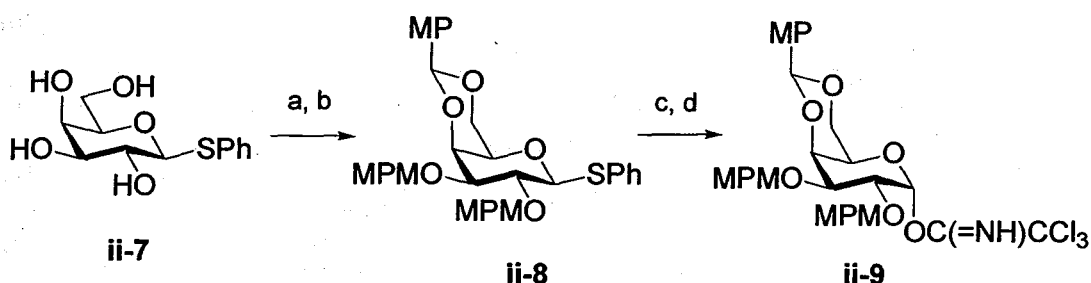


**Scheme ii-1. Reagents and conditions**

- (a)  $\text{TrCl}$ , Py,  $100^\circ\text{C}$ , 73%.
- (b)  $\text{BzCl}$ , Py,  $\text{CH}_2\text{Cl}_2$ ,  $0^\circ\text{C}$ , 95%.
- (c)  $\text{AcOH}$ ,  $\text{H}_2\text{O}$ ,  $60^\circ\text{C}$ , 75%.
- (d) TEMPO,  $\text{PhI}(\text{OAc})_2$ ,  $\text{CH}_2\text{Cl}_2$ ,  $\text{H}_2\text{O}$   
then  $\text{CH}_2\text{N}_2$ ,  $\text{Et}_2\text{O}$ , 95%, 2 steps.

Glycosyl donor **ii-9** was also synthesized from phenyl 1-thio- $\beta$ -D-galactopyranoside (**ii-7**) as shown in **Scheme ii-2**.<sup>17</sup> After the C4 and C6 alcohols in **ii-7** had been simultaneously protected in the form of *p*-methoxyphenylmethyldene acetal,<sup>18</sup> the remaining C2 and C3 alcohols were

transformed into MPM ethers with MPMBBr/NaH to afford **ii-8** in 69% yield in two steps. Treatment of **ii-8** with NBS under the aqueous condition hydrolyzed the phenylthio acetal to provide the corresponding hemiacetal, which was further converted into  $\alpha$ -trichloroacetimidate **ii-9** according to Schmidt's protocol.<sup>19</sup>

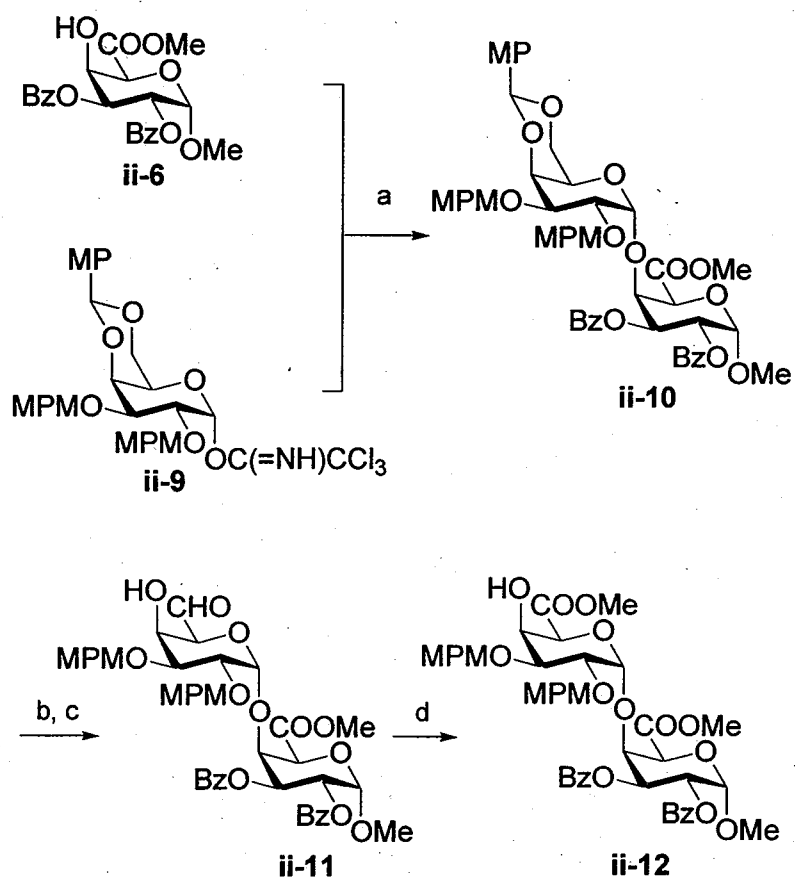


**Scheme ii-2. Reagents and conditions**

- (a) *p*-MeOPhCH(OMe)<sub>2</sub>, CSA, DMF, 100 °C, 72%.
- (b) MPMBBr, NaH, DMF, toluene, 96%.
- (c) NBS, acetone, H<sub>2</sub>O, 0 °C, 98%.
- (d) Cl<sub>3</sub>CCN, DBU, CH<sub>2</sub>Cl<sub>2</sub>, -15 °C, 89%.

Since my previous studies had revealed that the carboxylate ester function at the C6 position inhibited a glycosylation reactions,<sup>20</sup> the C6 carboxylic acid group was introduced after the glycosylation. As expected, **ii-9** smoothly reacted with acceptor **ii-6** by using catalytic TESOTf to stereoselectively give  $\alpha$ -glycoside **ii-10** in 73% yield (**Scheme ii-3**). The  $\beta$ -isomer was not found in the <sup>1</sup>H NMR spectrum. After the *p*-methoxyphenylmethyldene acetal had been selectively removed under the aqueous acidic condition, C6OH of the resulting diol was selectively oxidized under the same conditions to those described for the oxidation of **ii-5**. This oxidation did not provide the carboxylic acid, but only

aldehyde **ii-11**, so it was further oxidized into carboxylic acid with  $\text{NaClO}_2$ . After treating with  $\text{CH}_2\text{N}_2$ , dimethyl ester **ii-12** was obtained in 80% yield in three steps.



**Scheme ii-3. Reagents and conditions**

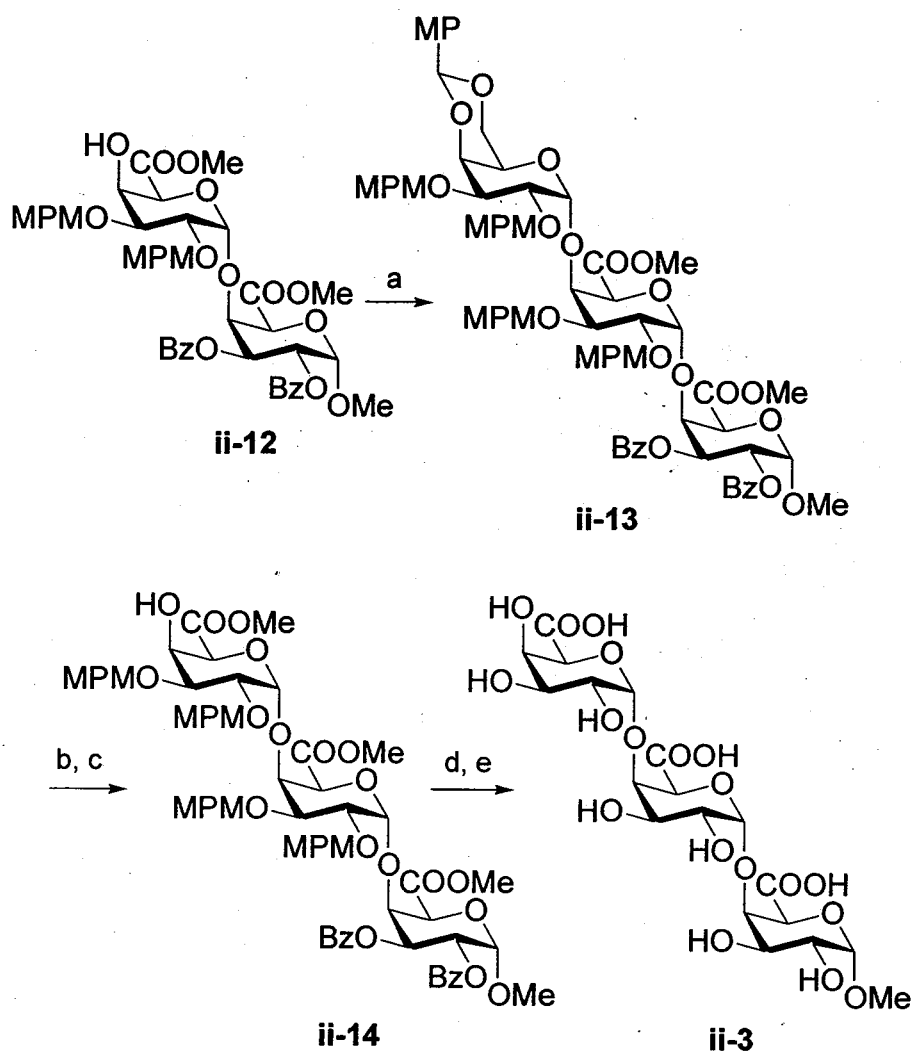
(a) TESOTf,  $\text{CH}_2\text{Cl}_2$ , MS4A,  $-78\text{ }^\circ\text{C}$ , 73%.

(b) AcOH,  $\text{H}_2\text{O}$ ,  $50\text{ }^\circ\text{C}$ , 92%.

(c) TEMPO,  $\text{PhI}(\text{OAc})_2$ ,  $\text{CH}_2\text{Cl}_2$ .

(d)  $\text{NaClO}_2$ ,  $\text{NaH}_2\text{PO}_4$ , *t*-BuOH, 2-methyl-2-butene then  $\text{CH}_2\text{N}_2$ ,  $\text{Et}_2\text{O}$ , 80%, 3 steps.

Product **ii-12** carried C4'OH, and this function was further glycosylated with **ii-9** under the same conditions to result in triglycoside **ii-13** with  $\alpha$ -stereochemistry (**Scheme ii-4**). The carboxylic acid function at the non-reducing end was provided by a similar sequence: (i) acidic removal of the *p*-methoxyphenylmethyldene acetal, (ii) TEMPO/PhI(OAc)<sub>2</sub> oxidation giving the corresponding C6 aldehyde, (iii) oxidation with NaClO<sub>2</sub>, and (iv) esterification with CH<sub>2</sub>N<sub>2</sub>. The last process, methyl ester formation, was required for effective silica gel column chromatographic purification. The MPM groups of **ii-14** were then removed by DDQ oxidation, giving the corresponding pentaol in 64% yield. Finally, a basic treatment under aqueous conditions removed all benzoate and methyl esters to achieve the synthesis of **ii-3** after passing the crude mixture through an ion-exchange column (Dowex 50W, H<sup>+</sup> form). My synthesis afforded a sufficient amount of **ii-3** (25 mg in total) for NMR and subsequent detailed calorimetric experiments.



**Scheme ii-4. Reagents and conditions**

(a) ii-9, TESOTf, Et<sub>2</sub>O, MS4A, 0 °C, 99%.

(b) AcOH, H<sub>2</sub>O, 50 °C, 79%.

(c) TEMPO, PhI(OAc)<sub>2</sub>, CH<sub>2</sub>Cl<sub>2</sub>

then NaClO<sub>2</sub>, NaH<sub>2</sub>PO<sub>4</sub>, *t*-BuOH, 2-methyl-2-butene,  
then CH<sub>2</sub>N<sub>2</sub>, Et<sub>2</sub>O, 68%, 3 steps.

(d) DDQ, CH<sub>2</sub>Cl<sub>2</sub>, H<sub>2</sub>O, 64%.

(e) 0.3% NaOH aq, THF, H<sub>2</sub>O, 98%.

## 2.3. Synthesis of sulfur-substituted analogue (**ii-1**)<sup>20</sup>

### 2.3.1. Design prior to the synthesis

The author designed **ii-1** as a stable mimic of natural substrate against endo-PG1. Prior to the synthesis, the author evaluated analogue **ii-1** by molecular dynamic simulations for the matrix of endo-PG1 and **ii-1** including 8633 waters.<sup>21</sup> These simulations suggested that analogue **ii-1** would bind to the enzyme in almost the same hydrogen-bonding manner (**Figure ii-4**) as the presumed native complex. The latter complex was constructed based on two X-ray structures, a complex with two galacturonic acids that bind at the subsites +1 and -1 individually, and a complex with a pentamer at subsite -1,-2,-3,-4. Although the substituting glycosidyl oxygen to sulfur did cause a minor conformational alteration, it did not greatly disturb the network of hydrogen bondings between the enzyme and the substance as shown in **Figure ii-4**. Accordingly, analogue **ii-1** would be an ideal molecular probe for mechanistic investigation.

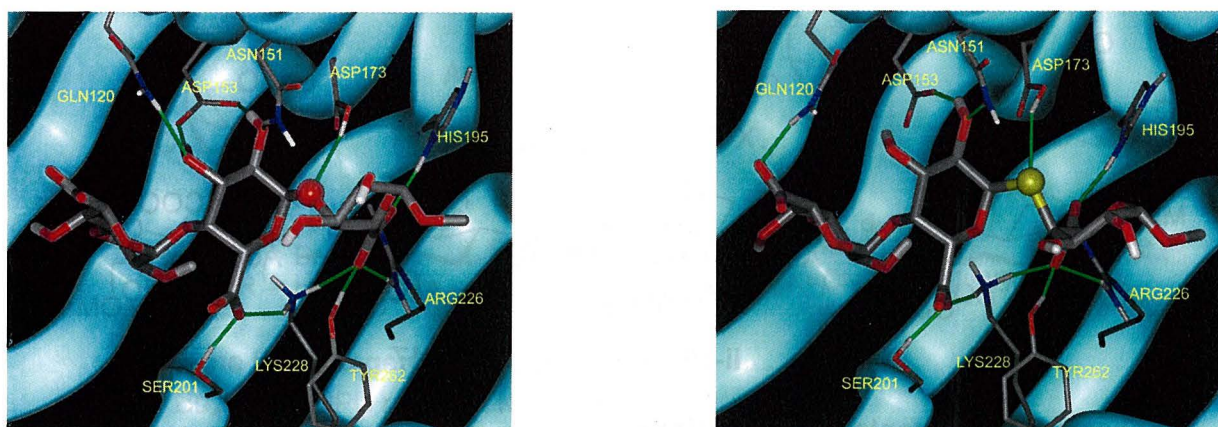
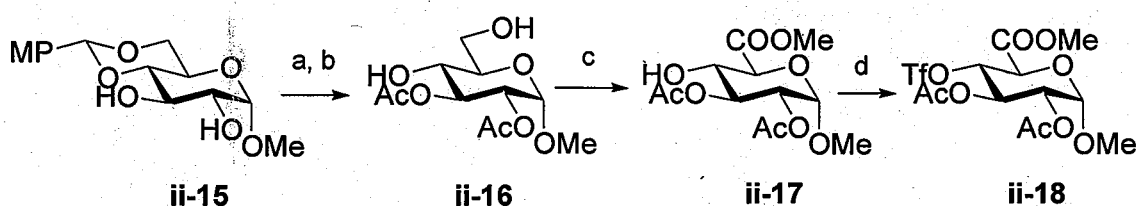


**Figure ii-4.** The matrix of endo-PG1 with natural substrate (left) and sulfur analogue **ii-1** (right) expected by the calculation using extended COSMOS90. The initial geometries were constructed based on the X-ray structure of endo-PG1 with galacturonic acids at subsites (+1,-1) and (-1,-2,-3,-4) obtained by the soaking experiments.

### 2.3.2. Synthesis

The author focused on introducing thioglycoside linkage by coupling 1-thioderivative **ii-25** with glucopyranose derivative **ii-18**, carrying a trifluoromethanesulfonate leaving group at the C4 position. My preliminary experiments suggested that the glycosylation of thiols using glycosyl trichloroacetimidates provided the desired glycoside only in low yields despite some successful reports.<sup>22</sup>

Triflate **ii-18** was first prepared as shown in **Scheme ii-5**. After acetylation of methyl 4,6-*O*-(4-methoxyphenylmethylidene)-glucopyranoside (**ii-15**),<sup>23</sup> the benzylidene moiety was removed by acetic acid to provide diol **ii-16** in 94% yield in two steps. Selective oxidation of the primary alcohol of **ii-16** was achieved by employing TEMPO and  $\text{PhI}(\text{OAc})_2$  under aqueous conditions. The following treatment with diazomethane gave methyl ester **ii-17** in 91% in two steps. The C4OH was then converted into sulfonate with  $\text{Tf}_2\text{O}$ /pyridine, giving **ii-18** in 94% yield.



#### Scheme ii-5. Reagents and conditions

(a)  $\text{Ac}_2\text{O}$ , Py, 98%.

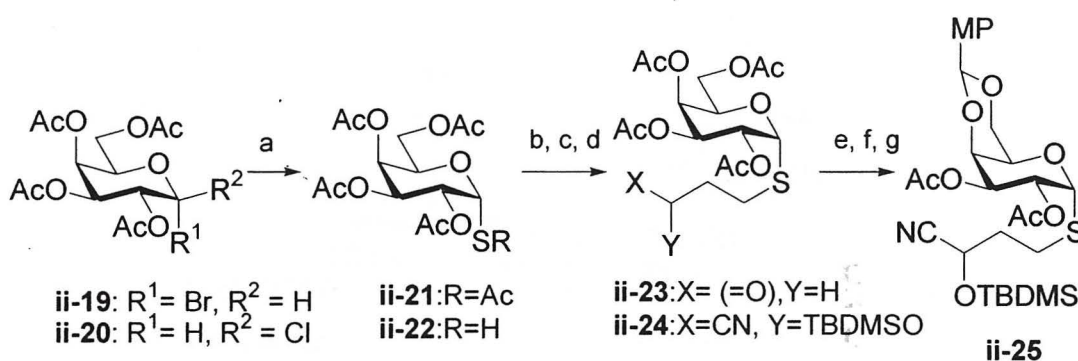
(b) AcOH,  $\text{H}_2\text{O}$ , 65 °C, 96%.

(c) TEMPO,  $\text{PhI}(\text{OAc})_2$ , acetone,  $\text{H}_2\text{O}$ , then  $\text{CH}_2\text{N}_2$ ,  $\text{Et}_2\text{O}$ , 91%.

(d)  $\text{Tf}_2\text{O}$ , Py,  $\text{CH}_2\text{Cl}_2$ , 94%.



The thiol part was then synthesized as shown in **Scheme ii-6**. The  $\alpha$ -thioacetyl group was introduced stereoselectively at the anomeric position via the double inversion of  $\alpha$ -galactosyl bromide **ii-19**. Treatment of **ii-19** with  $\text{Bu}_4\text{NCl}$  in DMPU at room temperature provided  $\beta$ -chloride **ii-20**,<sup>24</sup> which was further treated with potassium thioacetate using a one-pot procedure to give  $\alpha$ -thioacetate **ii-21** stereoselectively in 54% over all yield. Prior to manipulating 2,3,4,6-*O*-functions, the 1-*S*-acetyl group was replaced with a newly developed protective group, 3-cyano-3-*tert*-butyldimethylsilylpropyl (abbreviated to CSP group) thioether. The 1-*S*-acetyl group of **ii-21** was removed by basic methanolysis at  $-25\text{ }^\circ\text{C}$  to give thiol **ii-22** in 89% yield. Treatment of **ii-22** with acrolein (1.2 eq.) in DMF resulted in the Michael addition of thiol group. Following aqueous work-up, the aldehyde function in the resulting Michael adduct **ii-23** was further converted into *O*-silylated cyanohydrin by TBDMSCN

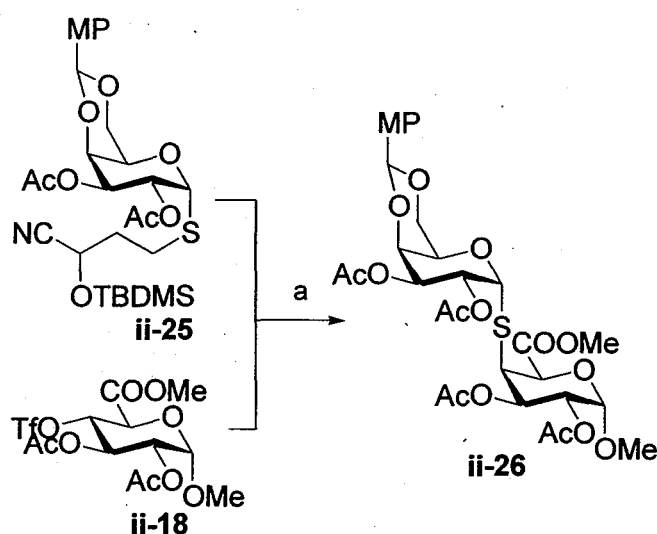


**Scheme ii-6. Reagents and conditions**

- (a)  $\text{Bu}_4\text{NCl}$ , DMPU r.t., then  $\text{KSAc}$ , 54%.
- (b)  $\text{NaOMe}$ ,  $\text{MeOH}$ ,  $-25\text{ }^\circ\text{C}$ , 85%.
- (c) acrolein,  $\text{DMF}$ .
- (d)  $\text{TBDMSCN}$ ,  $\text{KCN}$ ,  $\text{CH}_3\text{CN}$ , 73%, 2 steps.
- (e)  $\text{NaOMe}$ ,  $\text{MeOH}$ .
- (f)  $p\text{-CH}_3\text{O-PhCH(OCH}_3)_2$ ,  $\text{CSA}$ ,  $\text{DMF}$ , 69%, 2 steps.
- (g)  $\text{Ac}_2\text{O}$ ,  $\text{Py}$ , 93%.

in the presence of KCN in CH<sub>3</sub>CN to provide **ii-24** in 73% yield in two steps. The <sup>1</sup>H NMR spectrum indicated that **ii-24** was a 1:1 mixture of diastereomers regarding the cyanohydrin moiety. This protective function was found to be stable during the following treatments. After all acetyl groups in **ii-24** were removed by basic hydrolysis, the C4 and C6OH were protected in the form of *p*-methoxybenzylidene acetal under the usual conditions. The remaining C2 and C3 alcohols were acetylated again to provide **ii-25** in good over all yields.

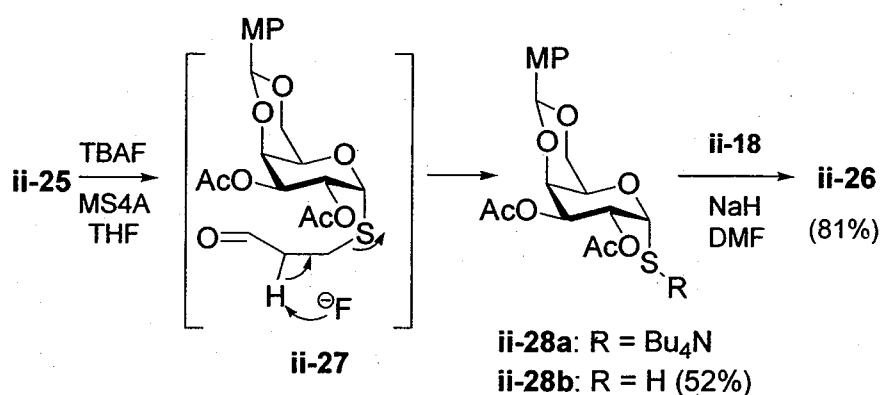
Treatment of **ii-25** with tetrabutylammonium fluoride in THF in the presence of molecular sieves 4A and the following addition of triflates **ii-18** after 5 min resulted in a coupling reaction to provide thioglycoside **ii-26** in 95% yield (Scheme ii-7).



**Scheme ii-7. Reagents and conditions**

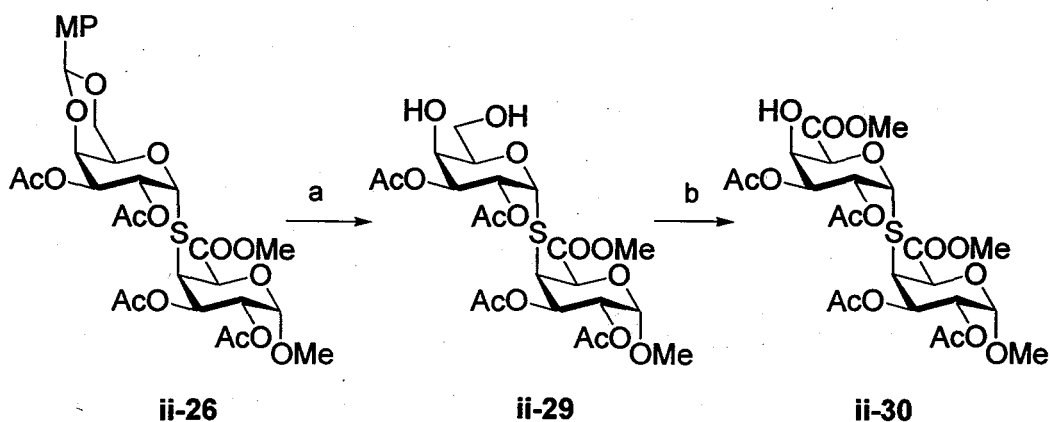
(a) TBAF, MS4A, THF, 95%.

The fluoride ion under aprotic conditions induced the *retro*-Michael reaction of regenerated aldehyde **ii-27**, giving **ii-28a** in a form of highly reactive tetrabutylammonium mercaptide. This method was more efficient than the stepwise transformations. Aqueous work-up prior to the addition of **ii-18** gave thiol **ii-28b** in 52% yield (Scheme ii-8). The basic treatment of pure **ii-28b** with TBAF/MS4A gave **ii-26** in only a 47% yield. Notably, the coupling reaction with pure **ii-28b** proceeded more smoothly to give **ii-26** in 81% yield by employing sodium hydride as the base.



Scheme ii-8.

Glycoside **ii-26** was then converted into glycosyl acceptor **ii-30** by i) acidic cleavage of the 4-methoxybenzylidene acetal ( $\rightarrow$ **ii-29**, 90% yield), oxidation of the primary alcohol with TEMPO/PhI(OAc)<sub>2</sub> followed by treatment with CH<sub>2</sub>N<sub>2</sub> ( $\rightarrow$ **ii-30**, 67% yield).

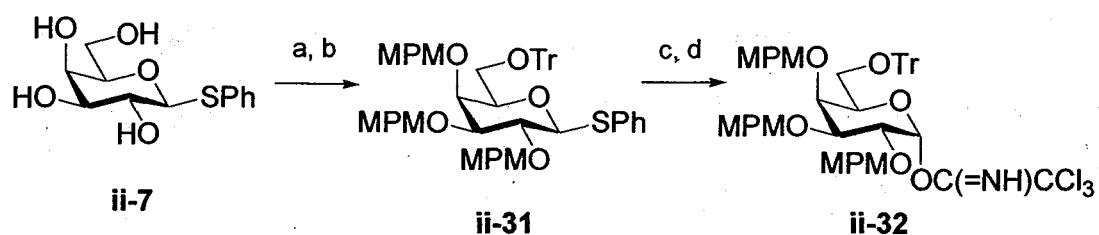


**Scheme ii-9. Reagents and conditions**

(a) AcOH, H<sub>2</sub>O, 65 °C, 90%.

(b) TEMPO, PhI(OAc)<sub>2</sub>, CH<sub>2</sub>Cl<sub>2</sub>, H<sub>2</sub>O, then CH<sub>2</sub>N<sub>2</sub>, Et<sub>2</sub>O, 67%.

Glycosyl donor **ii-32** was synthesized from phenyl 1-thio-β-D-galactopyranoside (**ii-7**) (Scheme ii-10). After tritylation of the C6 primary alcohol in **ii-7**, the remaining alcohols were transformed into MPM ethers with MPMBBr/NaH to afford **ii-31** in 70% yield in two steps. Treatment of **ii-31** with NBS under the aqueous condition hydrolyzed the



**Scheme ii-10. Reagents and conditions**

(a) TrCl, Py, 100 °C, 97%.

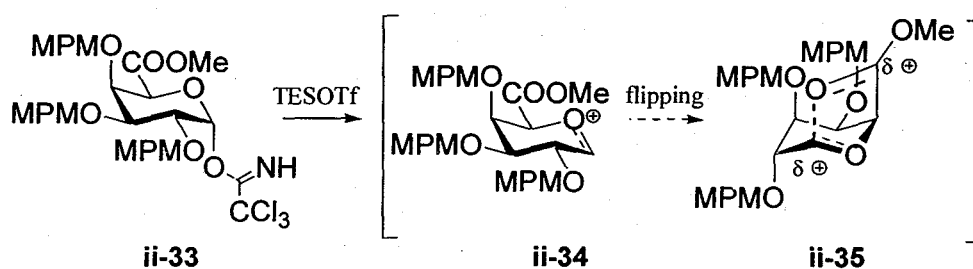
(b) NaH, MPMBBr, DMF, toluene, 72%.

(c) NBS, acetone, H<sub>2</sub>O, 0 °C, 99%.

(d) Cl<sub>3</sub>CCN, DBU, CH<sub>2</sub>Cl<sub>2</sub>, -15 °C, 99% (α:β = 5:1).

phenylthio acetal to provide the corresponding hemiacetal, which was further converted into  $\alpha$ -trichloroacetimidate **ii-32** according to Schmidt's protocol.

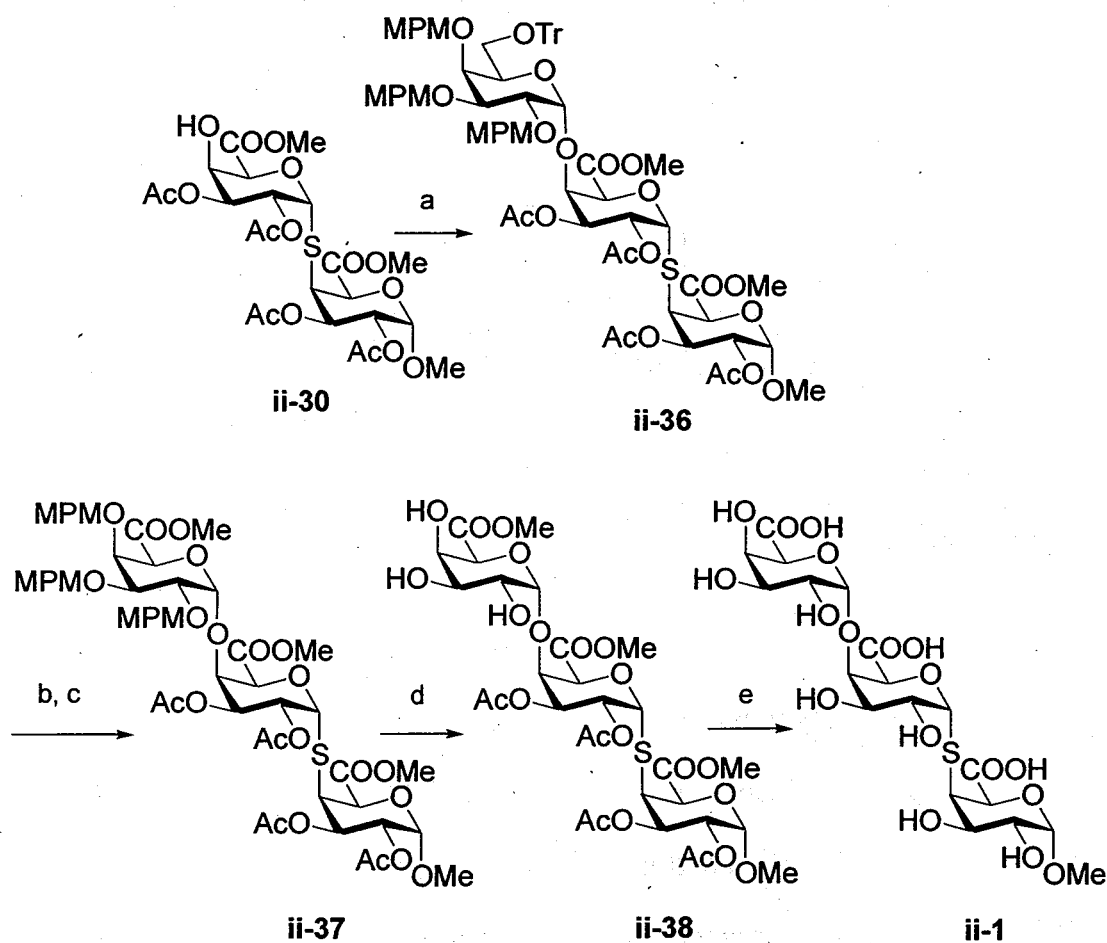
The author failed in the glycosylation of **ii-30** when galacturonate **ii-33** (Scheme ii-11)<sup>16, 25</sup> was employed as the donor although the glucuronate derivative (the C4 equatorial isomer) gave the adduct under the same conditions. Carbenium ion **ii-34** produced from **ii-33** was likely deactivated by the C6 carbonyl group after flipping the pyranose ring. Thus, we decided to construct the carboxyl group at the non-reducing end after glycosylation.



Scheme ii-11.

As expected, glycosylation of acceptor **ii-30** with trityl ether protected imidate **ii-32** took place to produce trimer **ii-36** stereoselectively in 72% yield by employing TESOTf as the activator (Scheme ii-12).<sup>19</sup> Stereochemistry of **ii-36** of the newly furnished glycoside bond was confirmed by observing the small coupling constants between C1'H and C2'H ( $J = 1.5$  Hz). The trityl ether in **ii-36** was selectively cleaved by aqueous acetic acid at 60 °C in 80% yield. Oxidation with TEMPO/PhI(OAc)<sub>2</sub> was also effective, and was followed by treatment with diazomethane to provide methyl ester **ii-37** in 98% yield in three

steps. Finally, all protective groups of **ii-37** were removed. The MPM ethers were cleaved by DDQ oxidation without declining the sulfide function<sup>26</sup> to give triol **ii-38** in 90% yield. The following basic treatment hydrolyzed all ester groups. Ion exchange column chromatography (Dowex 50W, H<sup>+</sup> form) after the reaction provided a pure sample of **ii-1** as a white powder.



**Scheme ii-12 Reagents and conditions**

- (a) **ii-32** TESOTf, CH<sub>2</sub>Cl<sub>2</sub>, -78 °C, 73%.
- (b) AcOH, H<sub>2</sub>O, 60 °C, 80%.
- (c) TEMPO, PhI(OAc)<sub>2</sub>, CH<sub>2</sub>Cl<sub>2</sub>, H<sub>2</sub>O, then CH<sub>2</sub>N<sub>2</sub>, Et<sub>2</sub>O, 98%.
- (d) DDQ, CH<sub>2</sub>Cl<sub>2</sub>, H<sub>2</sub>O, 90%.
- (e) NaOH, THF, H<sub>2</sub>O, 99%.

### 2.3.3 Biological property of sulfur substituted analogue

Preliminary enzymatic studies revealed that **ii-1** inhibited hydrolysis of oligo-galacturonic acid by endo-PG1 and was stable under these conditions. The experiments employing surface plasmon resonance revealed the  $K_D$  value of **ii-1** to be  $0.2 \mu\text{mol/L}$  (**Figure ii-5**).<sup>27</sup>

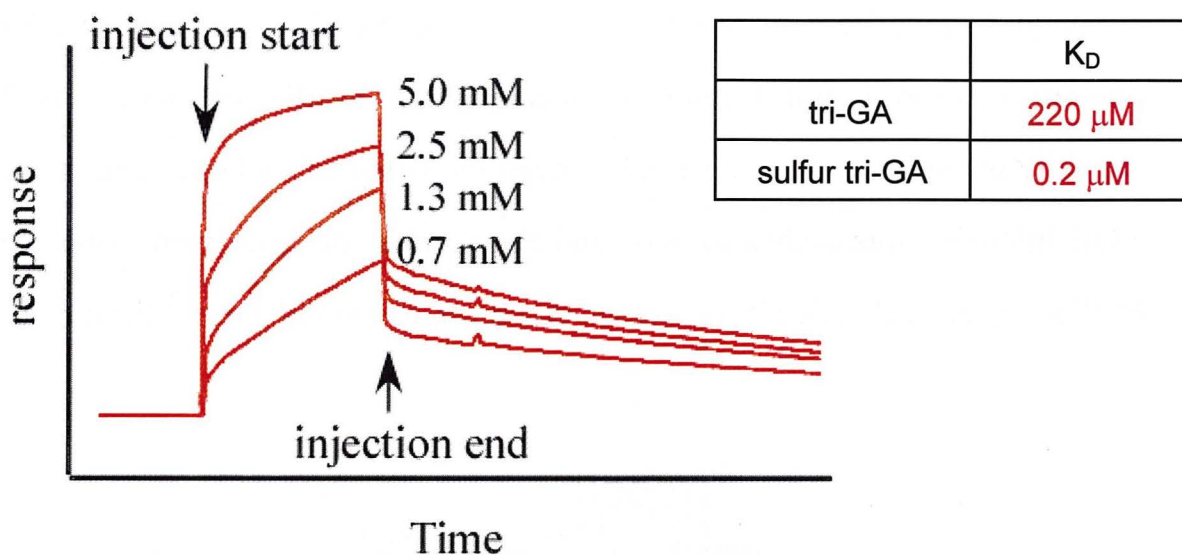


**Figure ii-5.** Stability of the complex with Biacore® (Surface Plasmon Resonance)

### 2.3.4. Conformational analysis

A preliminary conformational analysis of **ii-1** and **ii-3** was carried out by NMR experiments. NOESY is a powerful tool to investigate distances between two proton atoms.<sup>28</sup> In the carbohydrate research field, this technique has enabled the geometric-relationships of pyranose (or furanose) rings to be deduced in an oligosaccharide.<sup>29-31</sup> The 600-MHz NMR instrument provided the <sup>1</sup>H-NMR spectra for **ii-1** and **ii-3**, both with satisfying signal separation, although it gave very poor NOESY spectra. Generally, when the product of correlation time  $\tau$  and Larmor frequency  $\omega$  is small, the maximum NOE intensity is positive, while it becomes negative when  $\omega\tau_c$  is large. The maximum NOE intensity approaches to zero and the number of cross peaks observed in NOESY spectra drastically decreases when  $\omega\tau_c$  is around 1.13.<sup>32</sup> Fortunately, in

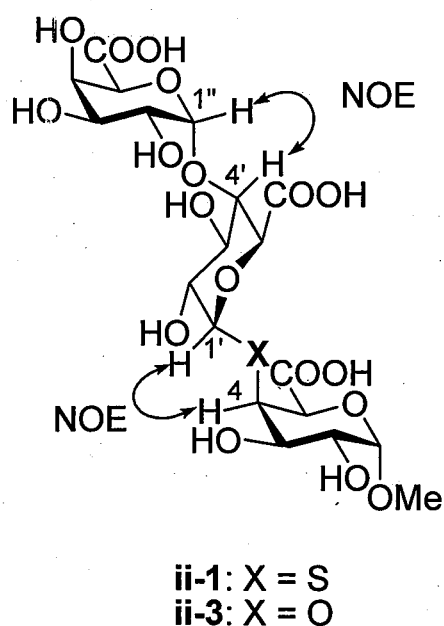


**Figure ii-6.** NOE correlations observed around the glycoside bond in **ii-1** and **ii-3**.



our case, a 920-MHz NMR spectrometer turned these invisible NOEs by the 600-MHz spectrometer into observable negative NOEs. There was no remarkable difference in the NOE pattern between **ii-1** and **ii-3**. Both compounds **ii-1** and **ii-3** afforded NOE correlations at  $1'' \leftrightarrow 4'$  and  $1' \leftrightarrow 4$  with similar intensity, suggesting that the glycoside bonds in each compound took on similar conformations (**Figure ii-6**).

This was also supported by molecular modeling calculations. The stable conformers for models X (*O*-glycoside) and Y (*S*-glycoside) were estimated by structural optimization with Hartree-Fock 6-31G\*<sup>33</sup> of the tentatively obtained stable conformers which were provided by a conformational search<sup>34</sup> with semiempirical AM1.<sup>35</sup>

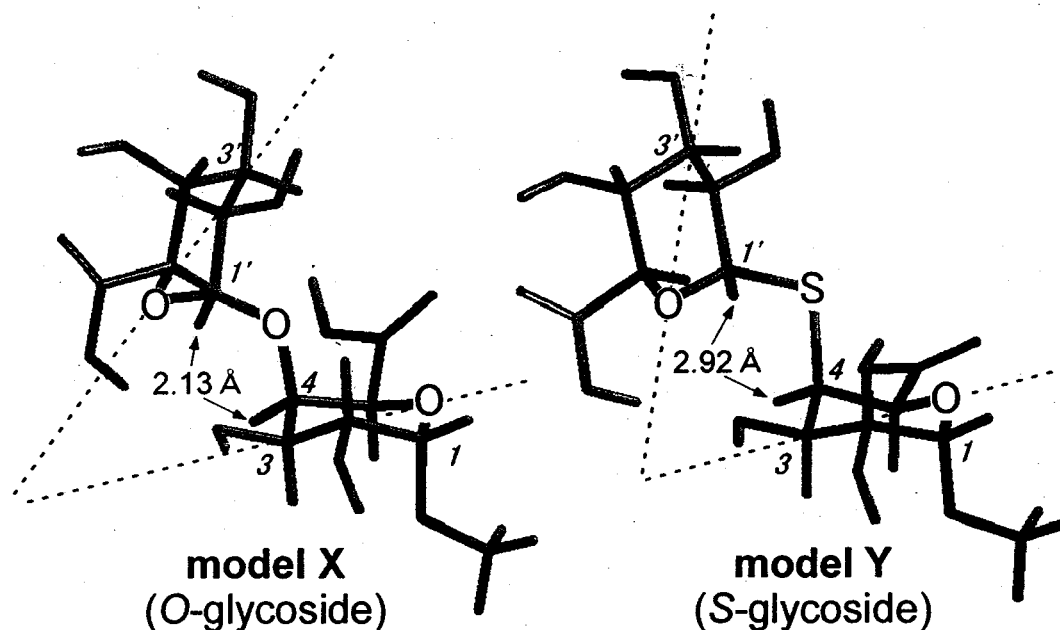


**Figure ii-7.** Stable Conformations of Models X (*O*-glycoside) and Y (*S*-glycoside) Obtained by Theoretical Calculations. The additional lines are those penetrating through pyranose oxygens and corresponding C3s.

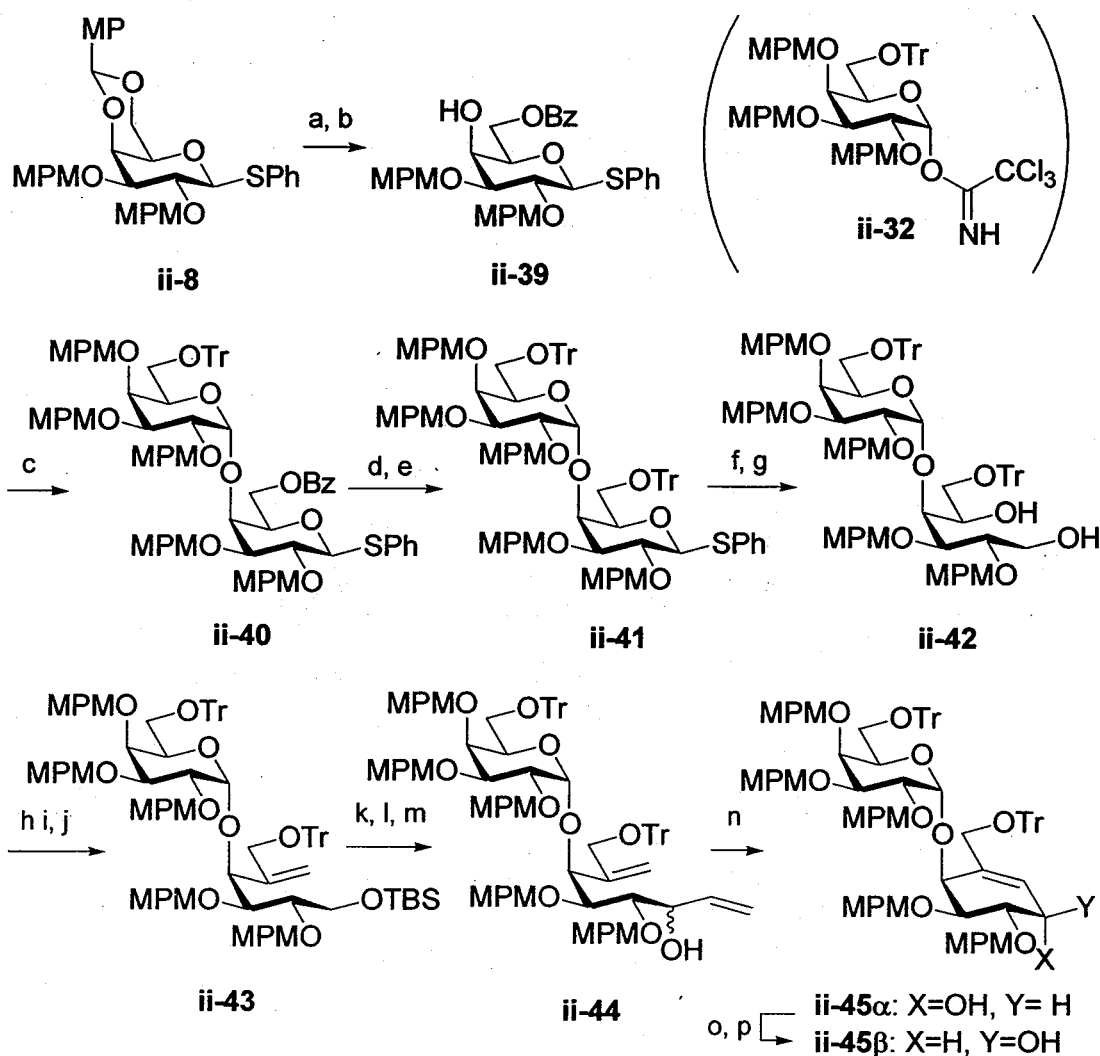
As shown in **Figure ii-7**, it was found that the pyranose rings in the stable conformers of models **X** (*O*-glycoside) and **Y** (*S*-glycoside) took on similar orientations. The distances between C4H and C1'H for both models **X** and **Y** were small, showing good accordance with experimental NOEs. However, that for model **Y** (2.92 Å) was larger compared to that for model **X** (2.13 Å), and the geometry of the pyranose rings was slightly different between models **X** and **Y**. Thus, I could conclude previously synthesized **ii-1** mimicked **ii-3** with slightly higher steric energy at the glycosyl bond being cleaved by endo-PG1.

## 2.4. Synthesis of transition state analogue (ii-2)

The author then attempted the synthesis the trigalacturonic acid analogue (ii-2) which carries a cyclohexene frameworks in place of the central pyranose ring of trigalacturonic acid. The cyclohexene ring was planed to be introduced by applying Halcomb's protocol employing ring closure metathesis with 2nd Grubbs' catalyst.<sup>36</sup>

Glycosyl acceptor **ii-39** was prepared from **ii-8** in good yield in two steps (Scheme ii-13). After the acidic hydrolysis of the 4-methoxybenzylidene acetal in **ii-8**, the regenerated primary alcohol was protected in a form of benzoyl ester to afford **ii-39** in 74% yield in two steps. The glycosylation of acceptor **ii-39** with trityl ether protected imidate **ii-32** by employing TESOTf as the activator provided di-saccharide **ii-40** in 92% yield as a mixture of  $\alpha$ - and  $\beta$ -glycosides ( $\alpha:\beta = 87:13$  by NMR). The diastereomers could not be separated by silica gel column chromatography, so the mixture was used for the next step. The benzoyl ester of **ii-40** was replaced with trityl ether by basic hydrolysis and the following treatment with TrCl/Py to afford **ii-41** in good yield. After basic hydrolysis of the benzoate ester, the diastereomers were readily separated by column chromatography. The resonance signal due to C1'H of **ii-41** appeared at 4.96 ppm as doublet ( $J = 2.5$  Hz) in the <sup>1</sup>H NMR spectrum, which confirmed the  $\alpha$ -stereochemistry of the glycosyl bonding newly formed by the glycosylation reaction. The phenylthio acetal of **ii-41** was hydrolyzed with NBS under aqueous condition to liberate the anomeric hydroxy group. Treatment of the product with sodium borohydride in ethanol took place the desired reduction to give diol **ii-42** in 92% yield in two steps. The diol **ii-42** was transformed into the olefin **ii-43** by i) selective protection of the primary alcohol of **ii-42** as the

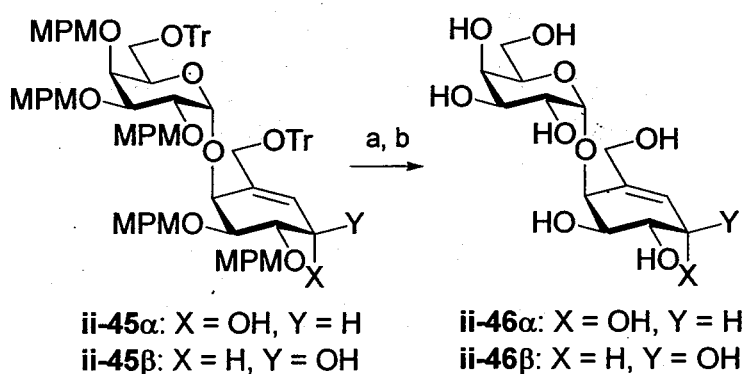
*tert*-butyldimethylsilyl (TBS) ether (98% yield), ii) oxidation of the secondary alcohol using DMSO/acetic anhydride (99% yield)<sup>37</sup> and iii) Tebbe olefination (65% yield).<sup>38</sup> After the TBS ether of **ii-43** was removed by TBAF, the resulting primary alcohol was oxidized to the aldehyde by Swern's condition<sup>39</sup>. Treatment of the aldehyde with vinylmagnesium bromide provided vinyl adduct **ii-44** in 81% yield in two steps. The <sup>1</sup>H NMR spectrum indicated that **ii-44** consisted with a 10:7 mixture of diastereomers at the C1 hydroxy moiety. After the cyclohexene ring was introduced by ring closure metathesis, these diastereomers were separated. The resulting diastereomeric mixture **ii-44** was treated with 4 mol % Grubbs' second-generation catalyst in toluene at 100 °C to afford cyclohexene **ii-45**. Medium pressured silica gel column chromatography separated the diastereomers, giving **ii-45 $\alpha$**  and **ii-45 $\beta$**  50 and 35% yield, respectively. The hydroxy group of  $\alpha$ -isomer **ii-45 $\alpha$**  was inverted by Mitsunobu reaction and subsequent basic hydrolysis to obtain the  $\beta$ -isomer **ii-45 $\beta$** .



### Scheme ii-13 Reagents and conditions

- (a) AcOH, H<sub>2</sub>O, 60 °C, 93%.  
 (b) BzCl, Py, CH<sub>2</sub>Cl<sub>2</sub>, 0 °C, 80%.  
 (c) **ii-32**, TESOTf, THF, MS4A, -20 °C, 92% ( $\alpha$ -isomer 82%,  $\beta$ -isomer 12%).  
 (d) 1M NaOH<sub>aq</sub>, MeOH, CH<sub>2</sub>Cl<sub>2</sub>, 74% (from diastereo mixture of **ii-40**)  
 (e) TrCl, Py, 70 °C, 98%.  
 (f) NBS, acetone, H<sub>2</sub>O, 0 °C.  
 (g) NaBH<sub>4</sub>, EtOH, CH<sub>2</sub>Cl<sub>2</sub>, 92% (2 steps).  
 (h) TBSCl, imidazole, DMF, 98%.  
 (i) DMSO, Ac<sub>2</sub>O, 99%.  
 (j) Tebbe reagent, toluene, Py, -40 °C  $\rightarrow$  0 °C, 65%.  
 (k) TBAF, THF, 97%.  
 (l) (COCl)<sub>2</sub>, DMSO, TEA, CH<sub>2</sub>Cl<sub>2</sub>, -78 °C.  
 (m) CH<sub>2</sub>CHMgBr, THF, -15 °C  $\rightarrow$  0 °C, 81%, 2 steps, (R:S=7:10).  
 (n) Grubbs II cat., toluene, 100 °C, 85% (**ii-45 $\alpha$**  50%, **ii-45 $\beta$**  35%).  
 (o) p-nitrobenzoic acid, DEAD, PPh<sub>3</sub>, THF, 0 °C  $\rightarrow$  r.t., 96%.  
 (p) 1M aq, NaOH, MeOH, CH<sub>2</sub>Cl<sub>2</sub>, 92%.

The stereochemistry of C1 position was determined after converting to **ii-46 $\alpha$**  and **ii-46 $\beta$** , because  $^1\text{H}$  NMR signal for critical proton was overlapped with other protons. The trityl group and MPM group were removed by acidic hydrolysis and DDQ oxidation, respectively (**Scheme ii-14**).



**Scheme ii-14 Reagents and conditions**

(a)  $\text{HCOOH}, \text{H}_2\text{O}, \text{MeOH}, \text{CH}_2\text{Cl}_2, 0\text{ }^\circ\text{C}$ .

(b)  $\text{DDQ}, \text{CH}_2\text{Cl}_2, \text{H}_2\text{O}$ , (**ii-46 $\alpha$** : 48%, **ii-46 $\beta$** : 55%, 2 steps).

In the  $^1\text{H}$ -NMR spectrum of **ii-46 $\alpha$** , small coupling constant between C1H and C2H (4.1 Hz) suggested gauche orientation. In contrast, that in **ii-46 $\beta$**  was 7.3 Hz to indicate quasi-anti relationship about C1H and C2H.

NOE experiments employing **ii-46 $\beta$** , irradiation of the signal for C3H (3.51 ppm, dd,  $J = 3.5, 10.6$  Hz) enhanced the resonance peak for C1H (3.97 ppm, brd,  $J = 7.3$  Hz), which indicated the cis-relationship between C1H and C3H. Irradiation of C1H also led on NOE at C3H to confirm this stereochemistry (**Figure ii-8**).

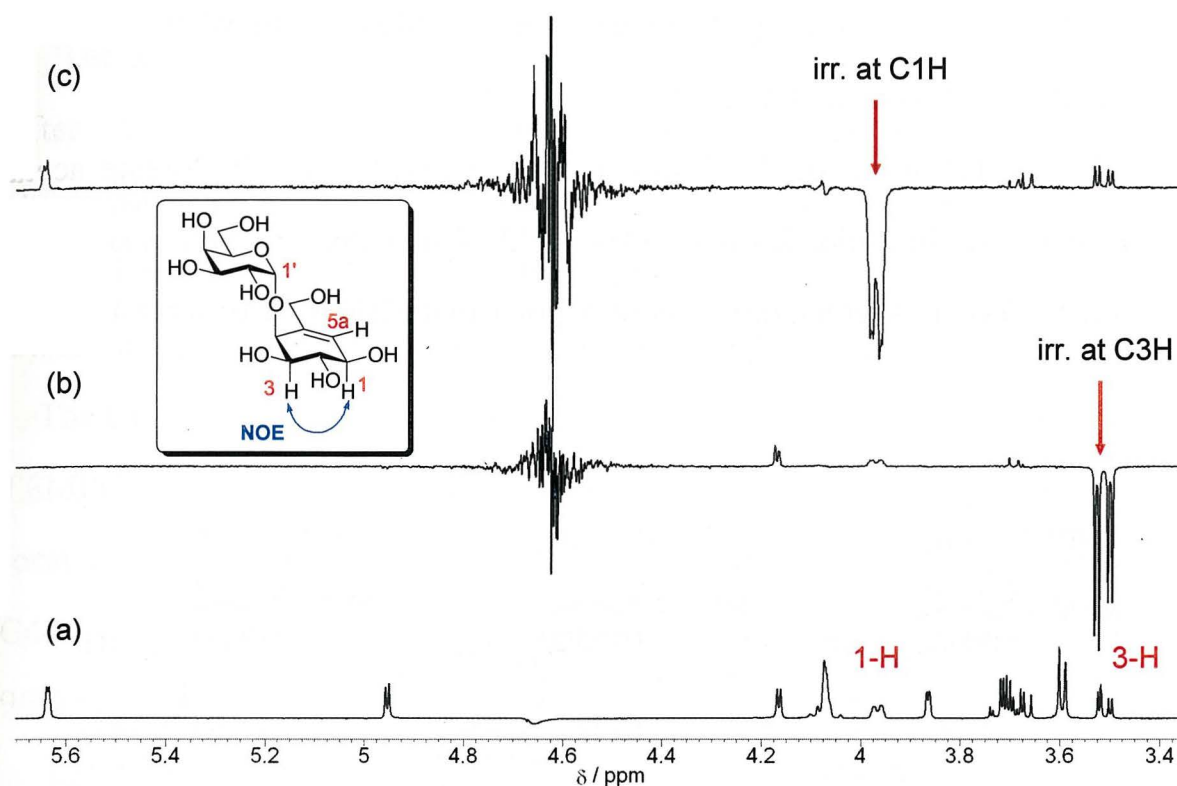


**Figure ii-8.** NOE correlation observed between C1H and C3H.

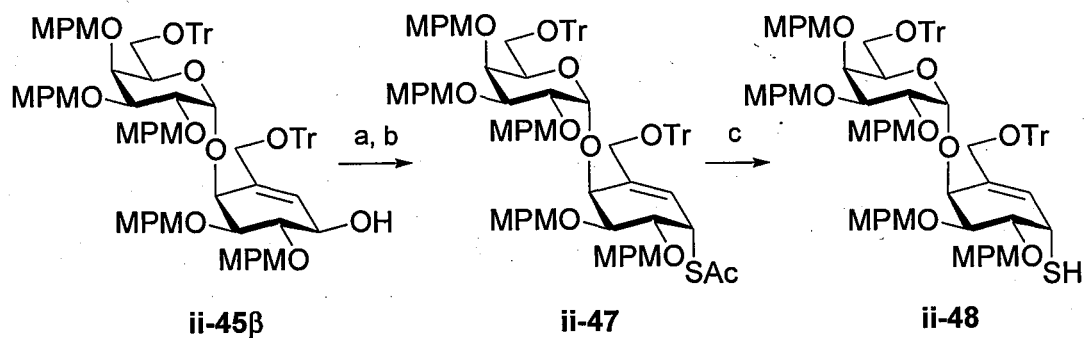
(a)  $^1\text{H}$  NMR spectrum of **ii-46**. (b) NOE spectrum of **ii-46** (irradiation at C3H). (c) NOE spectrum of **ii-46** (irradiation at C1H).

The  $\beta$ -hydroxy group of **ii-45 $\beta$**  was converted to  $\alpha$ -thioacetate **ii-47** (Scheme ii-15). Treatment of **ii-45 $\beta$**  with methanesulfonyl anhydride provided the corresponding  $\beta$ -mesylate,<sup>40</sup> which was further treated with potassium thioacetate without purification to afford  $\alpha$ -thioacetate **ii-47** in 98% in two steps.

Stereochemical inversion at the C1 position in this process was confirmed by observing small coupling constant (4.9 Hz) in the  $^1\text{H}$ -NMR spectrum. The  $\beta$ -isomer of **ii-47** was also prepared employing **ii-45 $\alpha$**  by the similar treatments. The coupling constant between C1H and C2H for this sample was 6.6 Hz in the

$^1\text{H-NMR}$  spectrum at  $50\text{ }^\circ\text{C}$  to indicate quasi-anti relationship for these protons. Interestingly the C1H signal appeared as broaden signal when the  $^1\text{H-NMR}$  spectrum was measured at  $25\text{ }^\circ\text{C}$ .

The acetyl group of **ii-47** was hydrolyzed with using hydrazine acetate in DMF to provide thiol **ii-48** in 84% yield. When this reaction was performed with NaOMe in MeOH, only complex polar materials were observed.



**Scheme ii-15 Reagents and conditions**

(a)  $\text{Ms}_2\text{O}$ , TEA,  $\text{CH}_2\text{Cl}_2$ ,  $-20\text{ }^\circ\text{C} \rightarrow 0\text{ }^\circ\text{C}$ .

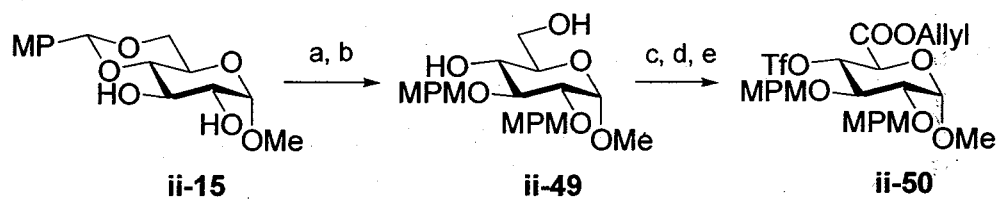
(b)  $\text{KSac}$ , DMF, 98% (2 steps).

(c)  $\text{NH}_2\text{NH}_2\text{AcOH}$ , DMF,  $0\text{ }^\circ\text{C} \rightarrow 10\text{ }^\circ\text{C}$ , 84%.



The key intermediate triflate **ii-50** was prepared as shown **Scheme ii-16**. After the C2 and C3OH of methyl 4,6-*O*-(4-methoxy)-benzylidene glucopyranoside **ii-15** were transformed into the corresponding bis-MPM ethers (81% yield), the *p*-methoxyphenylmethylidene acetal was selectively removed under the aqueous acidic condition giving **ii-49** in 96% yield.

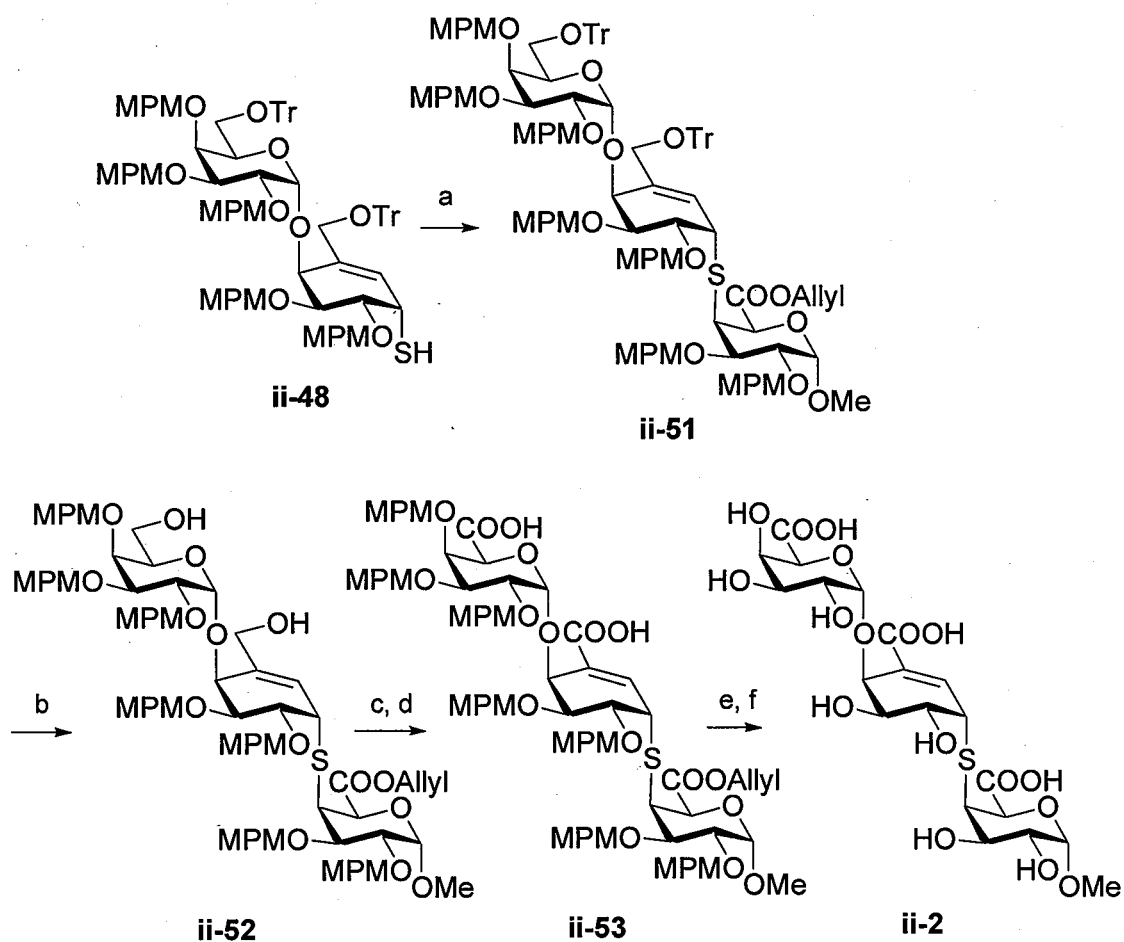
The C6 primary alcohol of **ii-49** was oxidized to carboxylic acid directly with TEMPO/PhI(OAc)<sub>2</sub> under aqueous conditions, which was then protected in the form of allyl ester with allyl alcohol/EDCI/HOBt in 57% in two steps. The C4-OH was then converted into sulfonate with Tf<sub>2</sub>O/pyridine, giving **ii-50** in 96% yield.



**Scheme ii-16 Reagents and conditions**

- (a) MPMBBr, NaH, DMF, 81%.
- (b) AcOH, H<sub>2</sub>O, 60 °C, 96%.
- (c) TEMPO, PhI(OAc)<sub>2</sub>, CH<sub>2</sub>Cl<sub>2</sub>, H<sub>2</sub>O, 84%.
- (d) allyl alcohol, EDCI, HOBT, CH<sub>2</sub>Cl<sub>2</sub>, 0 °C → r.t., 68%.
- (e) Tf<sub>2</sub>O, Py, CH<sub>2</sub>Cl<sub>2</sub>, 0 °C 96%.

With thiol **ii-48** and triflate **ii-50** in hand, the Williamson type coupling reaction of these two units was performed (**Scheme ii-17**). Sodium hydride mediated coupling smoothly proceeded to give triglycoside **ii-51** in 36% along with recovered thiol **ii-48** (41%). Thioglycoside **ii-51** was converted into dicarboxylic acid **ii-53** by (i) acidic removal of the trityl ethers ( $\rightarrow$ **ii-52**, 73% yield), (ii) Swern oxidation to give C6 aldehydes, (iii) oxidation with NaClO<sub>2</sub> ( $\rightarrow$ **ii-53**). Finally, all protective groups of **ii-53** were removed. Allyl ester was removed by using Pd(PPh<sub>3</sub>)<sub>4</sub>/pyrrolidine. All MPM ethers were then removed by the treatment with DDQ. After the unreacted DDQ and DDHQ were removed by EtOAc/H<sub>2</sub>O partition, ODS column chromatography provided **ii-2** in 90% yield in 4 steps. Since **ii-2** thus obtained involved small amount of impurity, HPLC purification (Inertsil<sup>®</sup> DIOL, 4.6×150 mm, H<sub>2</sub>O:CH<sub>3</sub>CN:TFA 10:90:0.01, 1.0 mL/min flow,  $t_R = 16$  min) was performed to afford the sample with enough purity for enzymatic experiments. The ESIMS gave the protonated molecular ion signal at  $m/z = 573.11240$  which proved oxidation of sulfide function did not occur during these processes. Preliminary enzymatic studies revealed that **ii-2** (0.3 mM solution) inhibited hydrolysis of tetra-galacturonic acid by endo-PG1 about 30%.



**Scheme ii-17 Reagents and conditions**

- (a) ii-50, NaH, DMF, 36%.
- (b) HCOOH, H<sub>2</sub>O, 0 °C → r.t., 73%.
- (c) (COCl)<sub>2</sub>, DMSO, TEA, CH<sub>2</sub>Cl<sub>2</sub>, -78 °C.
- (d) NaClO<sub>2</sub>, NaH<sub>2</sub>PO<sub>4</sub>, 2-methyl-2-butene, *t*-BuOH, H<sub>2</sub>O.
- (e) Pd(PPh<sub>3</sub>)<sub>4</sub>, Pyrrolidine, THF.
- (f) DDQ, CH<sub>2</sub>Cl<sub>2</sub>, H<sub>2</sub>O, 90% (4 steps).

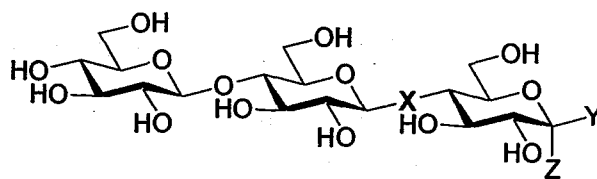
## **Chapter 3.**

### **Cellotriose analogues as molecular probes for mechanistic investigation of cellulase**

### 3.1. Introduction of this chapter

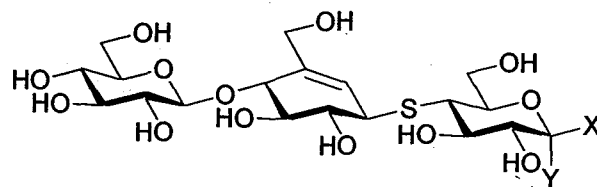
The author next applied synthesis of cellulose analogues. Nowadays, production of fuel ethanol depends on degradation of glucoses by fermentation. But it has lead serious increment of food prices in markets, because these industries mainly utilizes grain, corns, rice and wheat. Development of the effective methodology for cellulose/glucose process using cellulases would be ideal for production of ethanol from eatable by amylase, it enable us to utilize uneatable pulp, dead leaves, and grasses. In order to design effective and stable artificial cellulases for these industrial applications, understanding the detail reaction mechanism is indispensable to understand their functions by chemical functional levels. In order to provide effective tools for these studies, the author planed to synthesize the analogues for cellulase.

The author intends to elucidate the reaction mechanism of endoglucanase V. Endoglucanase V is one of cellulases, which is from *Humicola insolens*. Professor Kidokoro disclosed that the minimum size of substrate is trimer, and it is hydrolyzed at the reducing end. Methyl glycoside was introduced for each reductive terminal, since anomeric hydroxy group are readily epimerized to make thermochemical discussions difficult. The author synthesized both isomers to confirm that not only  $\beta$ -isomer (**iii-1b** and **iii-2b**) but also  $\alpha$ -isomer (**iii-1a** and **iii-2a**) could form the complex with endoglucanase V without hindrance (**Figure iii-1**).



**iii-1a:** X = S, Y = H, Z = OMe

**iii-1b:** X = S, Y = OMe, Z = H



**iii-2a:** X = H, Y = OMe

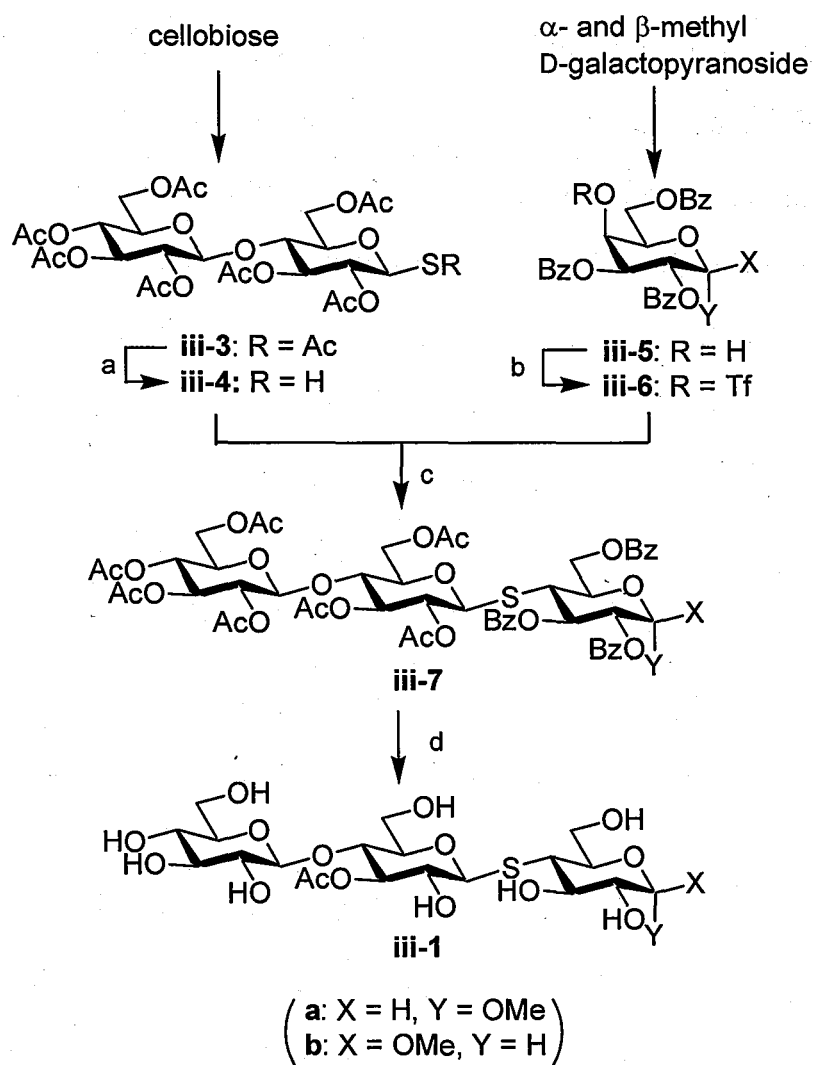
**iii-2b:** X = OMe, Y = H

**Figure iii-1.** Structures of celotriose analogues.

### 3.2. Syntheses of sulfur substituted analogues (**iii-1a** and **iii-1b**)

The sulfur substituted analogues (**iii-1a** and **iii-1b**) were synthesized as shown in **Scheme iii-1**. 1- $\beta$ -Thioacetylcellobiose heptaacetate **iii-3** was prepared from commercial cellobiose in good yield by reported procedure.<sup>41</sup> The thioacetyl group at the anomeric position was selectively removed by sodium methoxide in methanol at low temperature to give thiol **iii-4**. Then **iii-4** was coupled with **iii-6a** and **iii-6b** prepared from methyl  $\alpha$ - and  $\beta$ -D-galactopyranosides, respectively, by selective benzylation<sup>42, 43</sup> at ( $\rightarrow$ **iii-5**) followed by triflate formation. Thiolate formation from **iii-3** with NaH in THF effected the condensation to afford trimer **iii-7a** (73% yield) and **iii-7b** (67% yield), respectively. After removal of all ester groups in **iii-7a** and **iii-7b** by basic hydrolysis, ion exchange column chromatography (Dowex 50W, H<sup>+</sup> form) provided a pure sample of sulfur substituted analogue **iii-1a** and **iii-1b**.

The <sup>1</sup>H NMR spectra of **iii-1a** and **iii-1b** confirmed  $\beta$ -stereochemistries for the C4-C1' glycoside linkages being introduced in these synthesis on the bases large the coupling constants (both 8.0 Hz) and also confirmed that both samples had enough purities for further enzymatic studies.



**Scheme iii-1. Reagents and conditions**

(a) NaOMe, MeOH, -15 °C.

(b) Tf<sub>2</sub>O, Py, CH<sub>2</sub>Cl<sub>2</sub>, 0 °C.

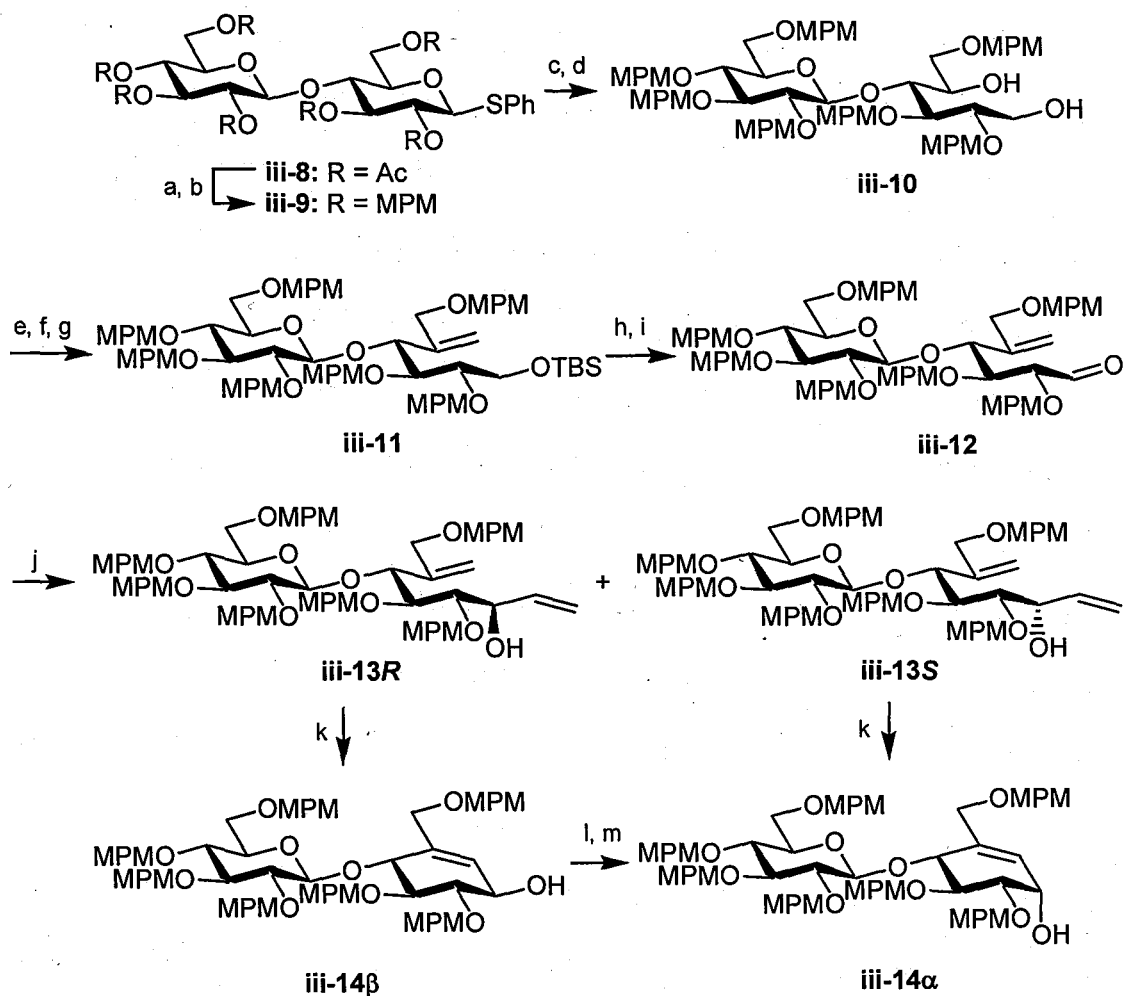
(c) NaH, THF, 0 °C, **iii-7a**: 73% (from **iii-3**), **iii-7b**: 67% (from **iii-3**).

(d) NaOH, MeOH, H<sub>2</sub>O, **iii-1a**: 99%, **iii-1b**: 98%.



### 3.3. Syntheses of transition state analogues (**iii-2a** and **iii-2b**)

Transition state analogues **iii-2a** and **iii-2b** carrying cyclohexene frameworks in place of the pyranose ring of celotriose were synthesized. The cyclohexene ring was constructed according to Halcomb's protocol with some improvements.<sup>36</sup> The synthesis commenced with known phenyl hepta-*O*-acetyl-1-thio- $\beta$ -D-cellobioside **iii-8** (Scheme **iii-2**).<sup>44</sup> The acetyl esters of **iii-8** were replaced with MPM ethers to afford **iii-9** in 73% yield by basic hydrolysis and the following treatment with MPMBR/NaH. Treatment of **iii-9** with NBS under aqueous conditions liberated the anomeric OH. The following reduction with sodium borohydride in ethanol gave diol **iii-10** in 99% yield in two steps. After protection of the primary alcohol as TBS ether (97% yield), *exo*-methylene was introduced by a sequential reactions of (i) Albright-Goldman oxidation<sup>37</sup> of the remained alcohol to the ketone and (ii) Wittig methylation employing methyltriphenylphosphonium bromide in 92% yield in two steps.<sup>45</sup> Tetrabutylammonium fluoride mediated desilylation provided the corresponding primary alcohol, which was further converted into the aldehyde **iii-12** by Swern oxidation<sup>39</sup> in 98% yield in two steps. Then, vinyl group was introduced by vinyl magnesium bromide to give 1:1 mixture of allylic alcohol **iii-13R** and **iii-13S** in 90% yield, which were successfully separated by medium pressured silica gel column chromatography. Stereochemistry of them were established after cyclization. These diastereomers **iii-13R** and **iii-13S** were then independently heated in the presence of 3 mol % Grubbs' second-generation catalyst<sup>46</sup> which took place the desired ring closure metathesis to afford cyclohexenols **iii-14 $\beta$**  and **iii-14 $\alpha$**  95 and 91% yield, respectively. Mitsunobu reaction and subsequent basic hydrolysis of **iii-14 $\beta$**  successfully inverted the OH group to converge to **iii-14 $\alpha$** .



### Scheme iii-2. Reagents and conditions

- (a) 2M NaOH, MeOH, CH<sub>2</sub>Cl<sub>2</sub>, 98%.
- (b) MPMBBr, NaH, DMF, 73%.
- (c) NBS, acetone, H<sub>2</sub>O.
- (d) NaBH<sub>4</sub>, EtOH, CH<sub>2</sub>Cl<sub>2</sub>, 99% (2 steps).
- (e) TBSCl, imidazole, DMF, 97%.
- (f) DMSO, Ac<sub>2</sub>O, 94%.
- (g) Ph<sub>3</sub>PCH<sub>3</sub>Br, n-BuLi, THF, 98%.
- (h) TBAF, THF, 99%.
- (i) oxalyl chloride, DMSO, Et<sub>3</sub>N, CH<sub>2</sub>Cl<sub>2</sub>, -78 °C, 99%.
- (j) CH<sub>2</sub>CHMgBr, THF, -15 °C, 90% (iii-13R: 46%, iii-13S: 44%).
- (k) Grubbs' II cat, toluene, 80 °C, iii-14α: 91%, iii-14β: 95%.
- (l) *p*-nitrobenzoic acid, DEAD, Ph<sub>3</sub>P, THF, 0 °C, 92%.
- (m) 2M NaOH, MeOH, CH<sub>2</sub>Cl<sub>2</sub>, 96%.

The stereochemistry of these products were determined after converting to the acetates **iii-15 $\beta$**  and **iii-15 $\alpha$** . Unfortunately specific NOE/ROEs were not detected, because both **iii-15 $\alpha$**  and **iii-15 $\beta$**  overlapped with benzyl protons due to the MPM groups. The C1H signal for **iii-15 $\beta$**  appeared 0.12 ppm lower frequency in the  $^1\text{H}$  NMR in  $\text{CDCl}_3$  than that of **iii-15 $\alpha$**  as shown in **Figure iii-2**. This suggested *pseudo*-axial geometry for the C1H of **iii-15 $\alpha$**  because of the magnetic shielding effect caused by the ring.<sup>47</sup> Large coupling constant (7.5 Hz) between C1H and C2H in **iii-15 $\beta$**  indicated that these protons were located in a *quasi*-antiperiplaner relationship. The coupling constant between C1H and C5aH was 1.2 Hz which suggested near to perpendicular relationship for the dihedral angle  $\angle\text{H-C5a-C1-H}$ . In the cases of **iii-15 $\alpha$** , the corresponding coupling constants  $^2J_{\text{C5aH-C1H}}$  and  $^2J_{\text{C1H-C2H}}$  were both 3.7 Hz, indicating gauche orientations for  $\angle\text{H-C5a-C1-H}$  and  $\angle\text{H-C1-C2-H}$ .

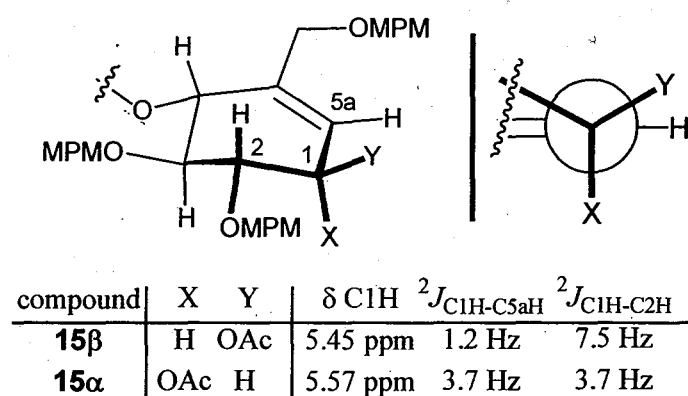
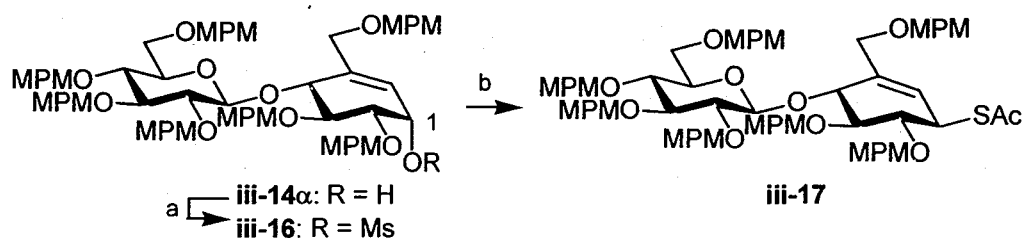


**Figure iii-2.** The chemical shifts and the coupling constants of the acetates **iii-15 $\alpha$**  and **iii-15 $\beta$** .

The  $\alpha$ -hydroxy group was converted to thioacetate **iii-17** stereoselectively via allylic mesylate **iii-16**<sup>48</sup> in 87% yield (Scheme iii-3). This transformation involved stereochemical inversion and **iii-17** thus obtained was a single diastereomer. Although this process was expected to proceed with stereochemical inversion, we needed confirm the stereochemistry of the product **iii-17**. Because mesylate **iii-16** might generate the stable corresponding allylic cation, allowing epimerization of **iii-16** and the  $\alpha$ -epimer should be more stable due to anomeric effect. It was determined after completion of the synthesis due to serious signal overlapping in the case of **iii-17**.

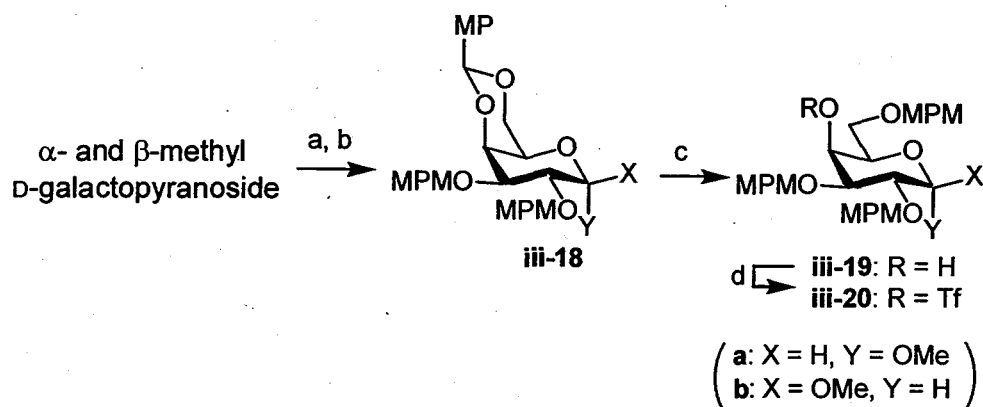


**Scheme iii-3. Reagents and conditions**

- (a)  $\text{Ms}_2\text{O}$ ,  $\text{Et}_3\text{N}$ ,  $\text{CH}_2\text{Cl}_2$ ,  $-15^\circ\text{C}$ .  
 (b)  $\text{KSAc}$ ,  $\text{DMF}$ ,  $0^\circ\text{C}$ , 87% (2 steps).

The coupling partners **iii-19a** and **iii-19b** were prepared both in good yields from methyl  $\alpha$ - and  $\beta$ -galactopyranoside, respectively, by (i) 4,6-*O*-(4-methoxybenzylidene)acetal formation, (ii) MPM ether protection of the C2 and C3 alcohols ( $\rightarrow$ **iii-18a**, **iii-18b**, respectively), and (iii) regioselective reductive cleavage of (4-methoxybenzylidene)acetal with  $\text{AlCl}_3/\text{BH}_3\text{NMe}_3/\text{MSAW}$  system (Scheme iii-4).<sup>49, 50</sup> The hydroxy groups of **iii-19a** and **iii-19b** were converted to trifluoromethanesulfonate esters to give

### iii-20a, iii-20b.



#### Scheme iii-4. Reagents and conditions

(a) MeOPhCH(OMe)<sub>2</sub>, CSA, DMF, 100 °C.

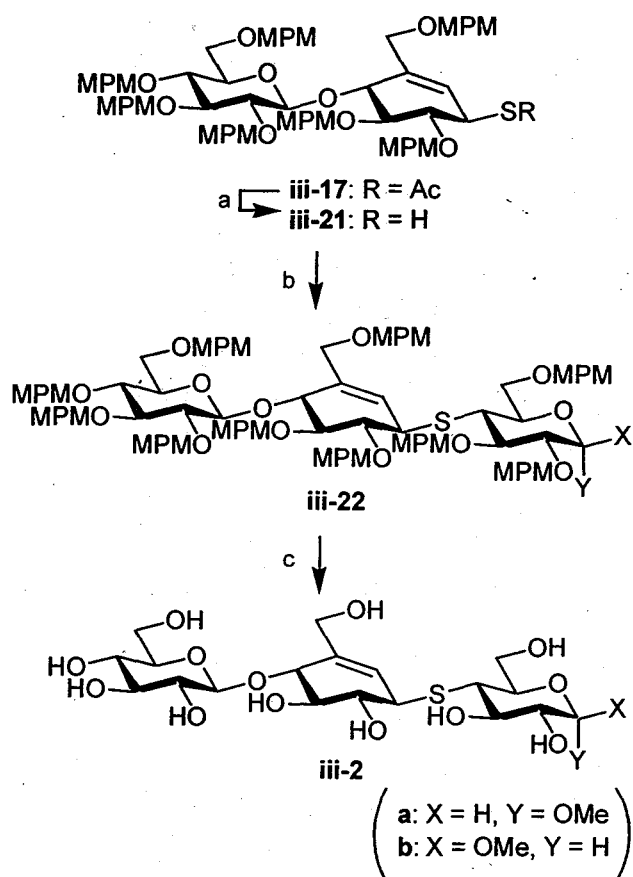
(b) MPMBBr, NaH, DMF, **iii-18a**: 66% (2 steps), **iii-18b**: 54% (2 steps).

(c) Me<sub>3</sub>NBH<sub>3</sub>, AlCl<sub>3</sub>, MSAW 300, THF, 0 °C, **iii-19a**: 57%, **iii-19b**: 66%.

(d) Tf<sub>2</sub>O, Py, CH<sub>2</sub>Cl<sub>2</sub>, 0 °C, **iii-20a**: 80%, **iii-20b**: 84%.

The coupling between the two segments **iii-21** and **iii-20** was then performed. Prior to the coupling, the thioacetate **iii-17** was converted into thiol **iii-21** by basic methanolysis (Scheme iii-5). Treatments of the sodium mercaptide derived from crude **iii-21** with crude triflates **iii-20a** and **iii-20b** in THF took place the couplings to give trisaccharide **iii-22a** and **iii-22b**. The yields were 55% and 58%, respectively, based on the amount of **iii-17** employed. Finally, all MPM ethers of **iii-22a** and **iii-22b** were removed by the treatment with DDQ. Since product **iii-2a** and **iii-2b** were soluble only in H<sub>2</sub>O, almost of unreacted DDQ and DDHQ formed in the reaction could be removed by EtOAc/H<sub>2</sub>O partition. Pure samples were obtained as white amorphous powder by lyophilization after ODS column chromatography. **iii-2a** and **iii-2b** was satisfying purity for the next

enzymatic investigation. The author has synthesized totally around 100 mg of samples.



**Scheme iii-5. Reagents and conditions**

- (a) NaOMe, MeOH, THF, 0 °C.  
 (b) iii-20, NaH, THF, 0 °C, iii-22a: 55%, iii-22b: 58%.  
 (c) DDQ, CH<sub>2</sub>Cl<sub>2</sub>, H<sub>2</sub>O, iii-2a: 87%; iii-2b: 89%.

Since the author could not discard the possibility giving more  $\alpha$ -epimer through the stable allylic cation as described in the synthesis for **iii-17**, the author needed to confirm the stereochemistry of final compound **iii-2**. It was found that the <sup>1</sup>H NMR spectrum peracetate **iii-23** in benzene-*d*<sub>6</sub> provided well

resolved the signals for observing NOEs, although crucial NOEs were not obtained because of signal overlapping in the cases either of **iii-2a** and **iii-2b** in D<sub>2</sub>O. The ROESY spectrum (mixing time = 300 msec) afforded the correlation signals between C1'H and C3'H, revealing the β-stereochemistry for the C1' position. Assignment of C1'H was performed by observing ROESY correlations with the C4H signal appeared characteristically lower frequency (2.84 ppm) due to the sulfur atom attached.

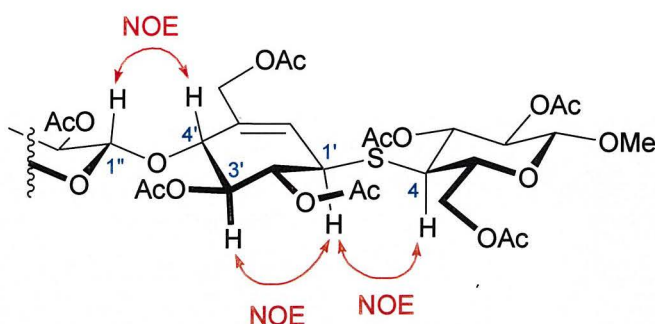


**Figure iii-3.** NOESY correlations and the stereochemistry of **iii-23**.